EA International

Lussebäcken, Helsingborg Municipality

Evaluation of the hydraulic performance of two-stage channels through comparative analysis – joint field-modelling approach

Lussebäcken two-stage channel, Site 1
Photos: EA International (March 2019)

Interreg North Sea Region Building with Nature
European Regional Development Fund

EUROPEAN UNION

Länsstyrelsen Skåne Län

Project Building With Nature (BwN)

February 2020

Report Number: 2020:05 (ISBN: 978-91-7675-184-8)

EA International

Lussebäcken, Helsingborg Municipality

Evaluation of the hydraulic performance of two-stage channels through comparative analysis – joint field-modelling approach

Prepared for: The County Board of Skåne (Länsstyrelsen Skåne Län)
Contact Person: Pär Persson
Report Number: 2020:05 (ISBN: 978-91-7675-184-8)

By:
Environmental Awareness International (EA International) • 24293 Hörby• Sweden
Contact: info@ea-international.se

Project scientist and lead	Jean O. Lacoursière, Ph.D.
Project scientist	Lena B.-M. Vought, Ph.D.
Project contract	4196005, Building with Nature WP4

and

DHI Sverige, Malmö • Södra Tullgatan 4, 3 vån • SE-211 40 Malmö • Sweden
Telefon: +46 10 685 08 00 • Fax: • info@dhi.se • www.dhi.se

Project Manager	Erik Mårtensson
Quality Supervisor	Ola Nordblom
Project Engineer	Christofer Karlsson
Project ID	12804393

Interreg North Sea Region Building with Nature European Regional Development Fund
EUROPEAN UNION

This work was supported as part of Building with Nature, an Interreg project supported by the North Sea Programme of the European Regional Development Fund of the European Union

Sammanfattning

En kvalitativ utvärdering gjordes för Lussebäckens avrinningsområde för de hydrauliska förändringarna som sker när ett jordbruksdike restaureras till ett tvåstegsdike genom simulering av en 1D hydraulisk modell (Mike Urban CS). Modellen kalibrerades och validerades genom att använda vattennivåmätningar från dataloggers samt parametrar från *in situ* konservativ spårämnesanalys (huvudsakligen medelhastighet och flöde för tvärsnittssektioner). De flesta trender och återkopplingar visas med den uppdaterade modellen, där det är en signifikant passning mellan modellerade och uppmätta parametrar. Förändringar i flöde, vattendjup, hastighet och hydraulisk retentionstid visas genom simulering där befintligt tvåstegsdike i Lussebäcken förändras till en trapetsoid form som är jämförbar med kontrollstationen som är ett jordbruksdike. Detta scenariot analyserades för simulerade full-bank ($Q_{1,5}$) förhållanden och med flödeshydrografer som togs fram vid den hydrologisk kalibreringsprocessen.

Simuleringen visade att, medan restaureringen inte minskat flödestoppen signifikant för tvåstegsdiken med en eller två översvämningsplan, förändringen från ett jordbruksdike till ett tvåstegsdike med två översvämningsplan minskar både vattendjup och flödeshastighet signifikant (i medeltal ca -35% respektive -160%) vid översvämning. Simuleringen med tvåstegsdiket med ett översvämningsplan visar på sämre prestanda även om en kombinerad påverkan av hög hydraulisk roughness samt hydraulisk kontroll nedströms gör det svårare att utvärdera. Simuleringarna visar också på en minskning av minst 50% av vattenhastigheten vid översvämning med översvämningsplan på båda sidor. Kombinationen av ökningen av den hydrauliska retentionstiden och reduktionen av vattenhastigheten minskar risken för kanterosion och sedimenttransport där näringsretentionen kan öka genom att sedimentpartiklar fångas upp och biogeokemiska processer ges mer tid. De simulerade ökningarna av vattendjup och flöde visar också att tvåstegsdike med två översvämningsplan minskar påverkan på dräneringsrör genom att minska mängden vatten som översvämmar in i rören.

Simuleringen lyfter fram att om tvåstegsdiket är byggt i ett område med låg lutning i bäckfåran, vegetation och sedimentackumulation i bäckfåran måste kontrolleras (öka hydraulisk roughness) för att minska vattendjupet vid högflöde. Finns det en damm nedströms kan vattendjupet påverkas genom nedströms hydraulisk kontroll.

Observationer gjorda i fält visar att även om volymmässigt, den hydrauliska lagringskapaciteten är stor, så passerar större delen av flödet i själva bäckfåran, där potentialen på översvämningsplanet inte utnyttjas (det uppskattades av endast 30% av det konservativa spårämnet som tillsattes vid punkt 0 hade nått översvämningsplanet efter 200 m). Detta gör att potentialen för sediment och näringsretention inte utnyttjas i översvämningsplanet till fullo, vilket visades i en studie som skedde parallellt. Förslaget är därför att testa, i gällande scenariot, åtgärder som ger ett jämnare flöde över hela översvämningsplanet för att öka sediment och näringsretention samtidigt som tvåstegsdikets hydrauliska prestanda (inkluderat en minskning av flödestoppen) upprätthålls. 1) minska växt-sediment feedback loop i bäckfåran genom att främja beskuggning av bäckfåran och översvämningsplanet i ett tidigt skedde 2) öka antal och längd av översvämningar genom att placera sten med intervaller i åfåran längs tvåstegsdiket 3) öka utbytet av vatten mellan bäckfåran och översvämningsplanet genom att placera deflektors (stockar, stenar) på översvämningsplanet vinklade på ett sådant sätt att vattnet sprids över hela översvämningsplanet.

Om minskningen av flödestoppen är huvudmålsättningen för att anlägga tvåstegdiken, föreslagna åtgärder i åfåran kan göras så att översvämningsplanen maximerar den volymmässiga lagringen (extended detention) men den effektivaste åtgärden är att anlägga en hydraulisk kontroll nedströms, t ex begränsa flödet genom en redan befintlig kulvert.

Även om den kalibrerade modellen för stationerna längs Lussebäcken visar bra trender och feedbacks för förhållanden som observerades under perioden kan ytterligare steg vara: 1) öka upplösningen på avvägningar i fält på longitudinella och tvärsnittsprofiler 2) använda olika hydrauliska roughness koefficienter under året för att fånga vegetationsförändringar, vilket kan göras genom konservativa spårämnesanalyser 3) använda en 2D modell istället för en 1D modell. Det har också visat sig att strömhastigheten uppmätt från spårämnesanalyser kan ersätta uppmätta vattendjup från dataloggers vid kalibrering av hydraulisk roughness i modellen.

Executive Summary

Qualitative assessment of the hydraulic changes associated with a two-stage channel approach to agricultural ditches restoration was performed through simulations of a 1D hydraulic model (Mike Urban CS) describing the Lussebäcken drainage basin. The model was calibrated and validated using site-specific water level recording and *in situ* conservative-trace derived parameters (mainly average cross-sectional velocity and discharge). Most trends and feedback are well captured by the updated model, with a significant fit between modelled and observed parameters achieved. Changes in discharge, water depth, velocity and hydraulic retention time are inferred from simulations where the actual Lussebäcken two-stage channels are returned to a trapezoidal cross-section similar to that of a nearby agricultural ditch reference site. This scenario was analysed under simulated full-bank flow ($Q_{1.5}$) condition and discharge hydrographs established through the hydrological calibration process.

Simulations demonstrate that, whilst it does not significantly attenuate peak-flow with one or two floodplains, restoring a trapezoidal drainage ditch to a two-stage two-floodplain channel significantly decreases both water depth and velocity (on average *ca.* -35% and -160% respectively) during overbank flow. Although obscured by the joint influence of high hydraulic roughness and downstream hydraulic control of the one-floodplain site, the simulation also indicates that performance is less with only one floodplain. Simulations also show that, during overbank flows, a minimum of 50% reduction in water velocity is provided by both floodplain configuration. In combination with the substantial increase in associated hydraulic retention time, velocity reduction potentially decreases risks of bank erosion and sediment transport, as well as promoting nutrient retention by increased particle trapping and time for biogeochemical processes. Furthermore, modelled change in water depth as discharge increases indicates that two-stage two-floodplain channel helps minimize the impact of high flows on the efficiency of underground drainage networks by reducing back-flow effect in outflow pipes. Simulations highlights that, if the restored reach has a shallow bed-slope, special attention must be provided to pro-actively control in-channel vegetation and sediment accumulation (*i.e.*, increased hydraulic roughness) to sustain water depth reduction performance. It also suggests that such performance would be even lower if a downstream pond is present (*i.e.*, downstream hydraulic control).

Field observations revealed that, although hydraulic storage is volumetrically significant, the great majority of the water rapidly flows downstream in the main-channel portion of the flooded cross-section of the two-stage channels, bypassing the full hydraulic resistance potential of the floodplains (*i.e.*, it was assessed that less than 30% of the conservative tracer released at the beginning of the two-stage channel travels over the floodplains by the time it reaches the 200m mark). This situation was identified as a significant hindrance to particle and nutrient retention potential by the parallel study. It is therefore suggested that the proposed interventions aimed at ensuring a more even flow-field distribution over the entire floodplains to promote particle and nutrient retention be tested in the existing scenarios to assess the extent they can also secure the two-stage channel designs hydraulic performance; which includes improving flow-peak attenuation. Recommended interventions are: **1)** supress in-channel plant-sediment feedback process by ensuring early shading of the main-channel and major parts of the floodplains; **2)** promote overbank flow frequency and duration by placing/keeping low-head structures such as riffle-pools or small woody debris-dams along the entire two-stage channel reach; and **3)** promote transversal mixing between the main-channel and the floodplains by securing deflectors on the bank, such as small/short tree logs, at an angle spreading the flow-field over the entire floodplain.

If flood-peak attenuation is the overriding objective in establishing a two-stage channel, whilst these recommended low-head structures (*e.g.*, riffle-pools, small woody debris-dams) could be optimized to maximize volumetric storage over the floodplains (*i.e.*, extended detention), the most effective approach is to explore the use of downstream hydraulic control (e.g., *outlet control* through reconfiguration of an existing culvert opening geometry).

Whilst the calibrated model of the Lussebäcken study-sites now captures quite well the trends and feedbacks over the whole range of conditions observed during the studied time period, it is suggested to: **1)** increase the resolution of the field surveys providing inputs on channel and floodplain longitudinal and cross-sectional profiles; **2)** consider using seasonal hydraulic roughness coefficient to represent vegetation changes – this could be done via conservative tracing; and **3)** use a 2D model instead of the current 1D model. It is also concluded that trace-derived velocities are good surrogates for automatically-recorded water depth in the calibration of hydraulic resistance in the model.

Table of Content

List of Figures

List of Tables

1 Preface

This report has been jointly prepared by EA-International and DHI Sverige AB in line with a directive from – and as part of their respective contracts with - *Länsstyrelsen Skåne*.

The respective tasks were for EA-International to generate field data to support the calibration & validation process of the *Lussebäcken* hydrological model performed by DHI Sverige AB. Initial coordination meetings, hosted by *Länsstyrelsen Skåne* (23rd Sept. & 23rd Oct. 2019), between the field and modelling teams resulted in adjustments of the respective contractual outcomes to better serve the project objectives under the available remaining time and resources. These adjustments were agreed by *Länsstyrelsen Skåne* and this report therefore only covers the actual outcome of these respective activities.

The report consists of an overall background and objective introduction, followed by two separate technical sections respectively on field and modelling activities, which is followed by a joint analysis of the two-stage channels performance with conclusions and recommendations.

2 Background

Agricultural land is in need of drainage trenches in order to optimize the productivity of the land. The traditional design of these ditches is a flat bottom with steep banks. Climate change entails measures of the watercourse to convey a higher discharge. At the same time, measures are essential to reduce nutrient leakage from agriculture and improve rural biodiversity. Restoration of rectified agricultural streams to two-stage channels is a viable management practice because it takes little land out of production, especially around many agricultural lands where grass buffer strips are already present. Once constructed, two-stage drainage requires little to no maintenance compared to the traditional trapezoidal channel. It is therefore a practice that easily co-exists with productive agriculture.

Two-stage channels are designed to mimic the stable conditions found in natural streams. The idea is to create extended benches on both sides of the rectified channel that would develop naturally over a period of time in a stream because of geomorphological processes. The shape of a two-stage channel varies slightly on a case-by-case basis, but typically consist of a low-flow trapezoidal channel, with capacity to convey the often-recurring hydrological conditions. On top of the banks of the low-flow channel, small vegetated benches on both sides are situated to serve as a floodplain. Where space is restricted, only one side of the channel can exhibit a floodplain. At high flow, typically every 1-2 years, full bank is reached and the floodplain used.

The primary design of a two-stage ditch is to reduce erosion along watercourses, so sediment in downstream watercourse is reduced. They also pose as a river restoration measure that recreates the humid environments that once existed along the watercourse. Vegetated benches further reduce water velocity at high discharge and moreover retain a greater proportion of sediments and nutrients in the watershed rather than be flushed out causing downstream problems.

2.1 Study-sites location and description

Since the end of the 1990s, the Municipality of Helsingborg in the southernmost province of Sweden (Skåne) has restored of a number of channelized agricultural streams to a more natural two-stage channel design. These were built as part of various nature-based measures (ponds, wetlands, buffer-zones) to reduce nutrient transport to the sea, increase agricultural biodiversity and decrease downstream flood-risk. Three of these sites along a

1,7 km stretch of the Lussebäcken, as well as an adjacent channelized tributary with traditional trapezoidal design set as a reference site, have been used in this study (Figure 1). Each of these sites is equipped with a stage recording station, where water depth data is available in nearly real-time through a web-based platform managed by an external consultant tasked to provide discharge-stage rating curves for each site. A 2018 geo-referenced survey of the four sites done by the Municipality of Helsingborg was provided to both field and modelling teams.

Figure 1 Map showing the relative locations of the four Lussebäcken study-sites, with positions of the automatic stage recorders and the Rhodamine WT injection & SCUFFA sites.

Study-description

For sake of clarity regarding their location along the Lussebäcken stream, the two-stage channel study-sites have been renumbered from their original BwN project labelling, with no. 1 reflecting the most upstream site.

Site 1 (BwN local 3) (Figure 2): well established two-stage channel created in 2002, with one floodplain on its left bank (facing downstream). It is today partially shaded by growing trees and shrubs (mainly alder *Alnus glutinosa* and willow *Salix spp*.) that have been planted or spontaneously established. The stream demonstrates low level of sinuosity and no real riffle-pool sections. The channel of the upper and lower sections can be heavily sedimented in place, while light to heavy in-channel vegetation (mainly cattail *Typha latifolia* and common reed *Phragmites australis*) is present on about 2/3 of its length. The grassy floodplain is partially covered by shrubs, which have been thinned-out a few times since. The hydraulic of the site's lower section is, at medium and high flows, significantly influenced by a downstream pond. The upper catchment is *ca*. 550 ha. Reach length is 204 m.

Figure 2 Study-site 1 (looking upstream, midway), a well-established two-stage channel restored in 2002. Photos: EA International (March 2019).

Site 2 (BwN local 2) (Figure 3): relatively young two-stage channel created at the end of 2015, with narrow floodplains boarded by a *ca.* 1:3 slope embankment. It is today fully exposed, with small shrubs starting to appear at some places along the edge of the floodplains. The entire channel is filled with sediment trapped by a very dense in-channel vegetation (mainly cattail *Typha latifolia* and common reed *Phragmites australis*) and the floodplains are dominantly un-vegetated. Consequently, water level is almost always at or above the designed full-bank and water flows more readily on the bare floodplains. The hydraulic of the site's lower section is, under all flows, significantly influenced by a densely vegetated reach. The upper catchment is *ca*. 650 ha. Reach length is 230 m.

Figure 3 Study-site 2 (looking upstream), a relatively young two-stage channel restored in 2015. Photos: EA International (March 2019).

Site 3 (BwN local 1) (Figure 4): well established two-stage channel created in 2002, with two floodplains. It is today heavily shaded by mature trees and shrubs (mainly alder *Alnus glutinosa* and willow *Salix spp*.), which were thinned out in the upper section's left bank near the end of the study period. The stream now demonstrates a marked sinuosity and harbour a floodplain on each side on most of its lower 2/3, with even a short parallel channel branch mainly active at high flows. Although some fine sediment deposits are present in the uppermost section, the channel bottom is dominated by gravel and fine sand, with some submerged vegetation (mainly the willow moss *Fontinalis antipyretica*).

Few real riffle-pool sections are present. At the exception of extremely high flows, the downstream free-flowing culvert (160 cm Φ x 12 m long pipe) does not really act as a significant hydraulic control. The upper catchment is *ca*. 750 ha. Reach length is 141 m.

Figure 4 Study-site 3 (looking upstream), a well-established two-stage channel restored in 2002. Photos: EA International (March 2019).

Site 4 (BwN local 4) (Figure 5): well established traditional agricultural ditch, *ca.* 2,5 m below field level with a *ca.* 1:1,4 slope embankment. It is today showing signs of heavy overgrowth, but close examination reveals that vegetation is dominantly from the side slopes. Both banks show signs of erosion at the same level, which could indicate the "full-bank" (1,5 year recurrence) flow mark. At medium and high flows, the downstream culvert (80 cm Φ x 59 m long pipe) can exert significant hydraulic control. The upper catchment is *ca*. 200 ha. Reach length is 213 m.

Figure 5 Study-site 4 (looking downstream), a well-established agricultural ditch showing signs of heavy overgrowth. A) close observation shows that vegetation is dominantly from the side embankment. Photos: EA International (August 2019).

The Lussebäcken drainage basin is a sub-catchment of the Råån river, which flows through the city of Helsingborg before it reaches the sea.

3 Study objectives and updated contractual outcomes

In following an update of the Lussebäcken sub-catchment in the hydrological model (Mike Urban CS) to better reflect prevailing land use and stormwater control measures, the main objective of this study was to establish the effect of a two-stage channel design on flood-risk reduction; more specifically on peak-flow magnitude, water depth and velocity, as well as hydrological storage potential.

To ensure reliability in findings, the updated hydrological model had to be first calibrated and then validated [DHI Sverige AB objective]. It was initially planned that this process would be based on flow-related Manning Roughness Coefficient (*n*, one of the key parameters involved in calibration/validation) derived from a conservative tracing field approach and a complementary desk software-based assessment [EA International objective]. However, discussions between the modelling and the field teams established that, based on the available time and resources, the most pragmatic approach to model calibration/validation was to directly use the average cross-sectional velocity (used in deriving *n*) determined by conservative-tracing. It was therefore decided that:

1) trace-derived Manning roughness coefficients would be used to guide/confirm the range of those employed in the model;
2) based on resources available, the desk-assessment of Manning *n* be abandoned in favour of extra traces; and,
3) although not initially considered, the calibration/validation process would also take advantage of the other parameters a conservative-trace generates; namely the prevailing flow-rate and cross-sectional dispersion coefficient.

Furthermore, because the provided geo-referenced survey resolution of the four sites was unfortunately insufficient to reliably obtain a trace-derived Manning roughness coefficient, an unplanned field-survey (5 cross-sections per site) had to be conducted by the field team. Consequently, these updated cross-sections were also incorporated in the final step of the calibration process to significantly improve the model fit. To further reduce discrepancies between modelled and observed water depths in the lower section of Site1 due to a hydraulic control associated with the downstream pond (Figure 1), this field survey also included the assessment of the prevailing difference in channel bottom and water surface heights between the end of Site 1 and the outflow of the pond.

Similarly, to strengthen and widen the flow-range on which the site's discharge rating-curves provided by Naturcentrum AB were based, a total of 40 (10 per site) complementary field-assessment of flows (Q) were also performed based on the Velocity-Area Method using an electromagnetic flow-meter. Final version of the 4 sites rating curves, which also includes trace-derived Qs, were therefore produced by the field team.

Finally, further discussions between the modelling and the field teams established that, in view of the significant variations in hydraulic behaviour amongst the two-stage channels at high flows due to unforeseen downstream hydraulic controls, as well as significant impact on channel geometry caused by substantial accumulation of sediment in some sites, it was decided that:

4) Site 2 would not be included in this modelling round;
5) the most effective way to achieve the objective of the project under the available time, was to apply the reference site's trapezoidal cross-section to the two-stage channel sites and infer the outcome of a restoration; and,
6) to apply this "reversal scenario" to sites 1 and 3 but, since it isn't influenced by hydraulic control at high flows, focus the assessment of the effect of two-stage channel mainly on Site 3.

The assessment of the two-stage channel restoration also included nutrient retention and local biodiversity (tasked to EA International) and is reported in a separate document. Similarly, flood-mapping of the entire Lussebäcken basin within the Råån hydrological model (tasked to DHI Sverige AB) is reported in a separate document.

4 Technical report on field activities [EA International]

4.1 Study Approach Rationale

As a low-gradient stream, the open channel flow in the selected reaches of Lussebäcken is essentially controlled by **(1)** *boundary roughness,* from bed and bank/floodplain grain material, including vegetation; **(2)** *form roughness,* from turbulences and secondary circulations generated channel irregularity and sinuosity; and, to a certain extent, by **(3)** *spill resistance*, induced by rapidly decelerating flows associated with hydraulic jumps induced by elements near or protruding from the water surface such as riffles. The later are potentially of importance at high flows since these structures promote over-bank flows. It is important to note that, as water flows under roads and pathways or enter/exit on-line ponds, *inlet/pipe control* **(4)** can also exert a significant control of the open-channel flow.

In modelling, the Gauckler-Manning-Strickler equation (simplify as Manning equation) is one of the most common mathematical constructs describing open channel flow:

$$Q = \frac{A\ R^{2/3}\ \sqrt{S}}{n} \qquad \text{Eq. 1}$$

where,

Q = flow rate (m^3/s);

A = area of channel perpendicular to the flow (m^2);

R = hydraulic radius (m), which is the variable accounting for the channel geometry:

$$R = \frac{A}{P} \qquad \text{Eq. 1b}$$

where,

P = wetted perimeter (m), the length of the channel perimeter in contact with the water.

S = average bed slope, as a surrogate for the energy grade line slope (m/m);

n = the "Manning coefficient" representing the "resistance" encountered by the flow. In Swedish literature, the inverse of n is used to depict this coefficient, with:

$$M = \frac{1}{n} \qquad \text{Eq. 1c}$$

While channel geometry and water/bed slope can easily be measured, estimation of a flow resistance coefficient (n) in natural channels (incorporating elements **1**, **2** and **3** above) remains an approximation and, depending on the method used, can be very subjective.

In this study, it was initially proposed to use two different approaches to estimate *n*:

A) a desk approach based on a multiple-steps spreadsheet tool developed by the U.S. Forest Service Natural Stream and Aquatic Ecology Centre to assist practitioners in selecting resistance coefficient for natural stream channels, through a combination of tabular and photographic guidance as well as quantitative approaches [In line with the agreed amendments (section 3), this approach was put on hold at this time]; *and*,

B) an *in situe* conservative-tracing approach to derive the roughness coefficient from field-assessed *"cross-sectional average velocity"* (V) and, using provided field-survey of the channel geometry (R and S) in the Manning equation solved for *n* :

$$n = \frac{R^{2/3}\ \sqrt{S}}{V} \qquad \text{Eq. 2}$$

In total, 39 traces were performed (min. 9 per site) and analysed to estimate associated cross-sectional velocity (V), flows (Q), dispersion coefficient (D) and derived Manning roughness coefficient (*n*).

4.2 Conservative-tracing – background and analysis

Soluble dye (such as the Rhodamine WT used in this study) has long been utilised to assess longitudinal transport and dispersion in free-flowing streams. Contrary to chemical or radioactive tracers requiring often costly laboratory analyses, florescence-tracing is now efficiently and economically performed using compact field-fluorimeters able to record at up to a 1 second sampling rate.

For small streams, the tracer is typically injected in a nearly instantaneous manner (slug-injection method) by pouring a set amount across the channel. Advection, dispersion and diffusion then stretch the tracer plug within the channel (and over the plains at flood stage) as it moves downstream. A monitoring instrument positioned at a set distance downstream from the injection would therefore detect a wave-like fluctuation in the tracer concentration as the marked water body passes-by. In its simplest form, this "breakthrough" (or dye recovery) curve would show a low concentration leading edge preceding the concentration peak, which is followed by a long trail of slowly decreasing concentrations until return to background fluorescence (Figure 6a). The higher the flow, the more diluted the tracer become. Similarly, the greater the "resistance" encountered by the flow, the more spread the curve becomes and the trail-end elongated.

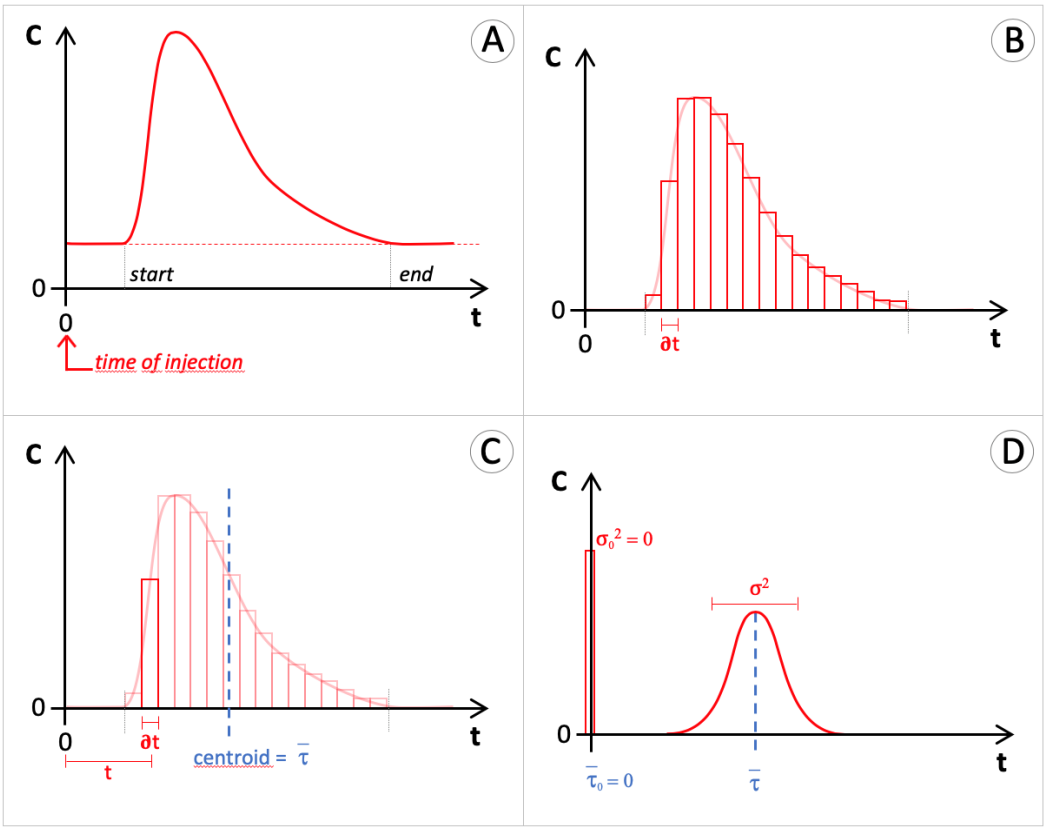

Figure 6 Graphics depicting the analysis of a breakthrough (dye recovery) curve generated by a conservative trace, with the x-axis representing time (s) and the y-axis Rhodamine WT concentration (ppb). A) removal of the background fluorescence and determination of the trace start & end; B) assessment of the dye "recovered" mass and determination of the prevailing water flow-rate; C) determination of the average travel time and the associated average cross-sectional velocity; and D) determination of the dispersion coefficient.

Because it involves hydrological processes applied to an entire reach, the information derived from a conservative trace are seen as reach-integrated; in contrast to punctual (location specific) readings of velocity, water depth, etc… collected by recording devices.

4.2.1 Trace Analytical procedure

From the breakthrough (dye recovery) curve generated by a conservative trace, where the x-axis is time (s) and the y-axis Rhodamine WT concentration (ppb), the flow-rate (Q) is defined as proportional to the area under the curve (Figure 6b), the average hydraulic travel time ($\bar{t}$) is expressed as the time where the centre of mass of the area under the curve is observed (Figure 6c), and the cross-sectional dispersion (D) proportional to the spread and trail-end (*i.e.*, the variance around $\bar{t}$; Figure 6d).

The sequential steps in analysing a breakthrough curve are:

1) Removal of the background fluorescence, which is an average of what was recorded prior to injection of the dye, must be performed before the actual concentration in Rhodamine WT (ppb) is computed from the relevant calibration equation (specific to an instrument) and the results plotted to identify the trace "start" and "end" time (Figure 6a).

2) Area under the curve is computed by making the summation of all individual areas associated with each recorded time interval (s) between the start and the end of the trace (Figure 6b). Representing the "recovered" dye, this "total mass" is annotated M_0 (the zeroth-moment of the distribution concentration over time) and has units of *ppb • S*:

$$M_0 = \sum_{start}^{end} c \cdot \partial t \qquad \text{Eq. 3}$$

where, "*c*" is the average of the actual concentrations observed at t_x and $t_{x+1.}$, respectively the beginning and the end of the time interval ∂t.

3) Flow-rate (Q) is determined based on a mass balance approach where the mass of the "recovered" dye is assumed to be equal to the mass that has been injected:

$$Q_{injection} \cdot PPB_{injected} = Q_{stream} \cdot PPB_{recovered} \qquad \text{Eq. 4}$$

Considering that the injection-rate was instantaneous, and therefore negligible in relation to the stream flow, the flow-rate is therefore equal to the ratio of the injected tracer mass (µg) and M_0, while the correction factor is used to account for the 20% active ingredient of the Rhodamine WT stock solution, as well as to bring the units to l/s.

$$Q_{stream} = \frac{PPB_{injected}}{M_0} \cdot (0{,}2 \cdot 1\,000\,000) \qquad \text{Eq. 4b}$$

4) Average travel time ($\bar{t}$) is determined by dividing the 1st Moment (M_1) of the distribution by its M_0, where M_1 is the summation of the multiplication of all individual "concentration masses" by their respective "time since injection" (t) (Figure 6c):

$$\bar{\tau} = \frac{M_1}{M_0} = \frac{\sum_{start}^{end} c \cdot t \cdot \partial t}{M_0} \qquad \text{Eq. 5}$$

where, "*c*" is the average of the actual concentrations observed at t_x and $t_{x+1.}$, respectively the beginning and the end of the time interval ∂t.

5) Average Cross-Sectional Velocity ($\bar{V}$) is calculated by dividing the distance (d) between the injection point and the reading instrument by $\bar{t}$:

$$\bar{V} = \frac{d}{\bar{t}} \qquad \text{Eq. 6}$$

6) The Dispersion Coefficient (D) is determined by first *assessing the variance about the centroid* ($\sigma_{\bar{t}}^2$) by dividing the 2nd Moment (M_2) of the distribution by its M_0:

$$\sigma_{\bar{t}}^2 = \frac{M_2}{M_0} = \frac{\sum_{start}^{end} c \cdot (t-\bar{t})^2 \cdot \partial t}{M_0} \qquad \text{Eq. 7}$$

And then by comparing the variance (σ_t^2) and centroid ($\bar{t}$)_of the injected and the "recovered" distributions related to the Average Cross-Sectional Velocity ($\bar{V}$) (Figure 6d):

$$D = \frac{U^2}{2} \cdot \frac{\sigma^2_{t_{trace}} - \sigma^2_{t_{injection}}}{\bar{t}_{trace} - \bar{t}_{injection}} \qquad \text{Eq. 8}$$

where, because the injection is instantaneous, $\sigma^2_{t_{injection}}$ and $\bar{t}_{injection}$ are equal to zero.

4.3 Conservative-tracing – field deployment and timing

Although 3 of the 4 study-reaches are along 1,7 km of the same channel stretch (only separated by *ca.* 530 m), pre-tests determined that the leading-edge of one trace would not overlap with the trail-end of another if individual / sequential traces were initiated from the downstream site, even if high concentration of Rhodamine WT were used.

To facilitate rapid-deployment, wood pegs were set in the middle of the channel at the beginning and end of each study sites; with the downstream one used to quickly anchor a SCUFA (Self-Contained Underwater Fluorescence Apparatus) (Figure 7b) and the upstream one to mark the dye injection point (Figure 7a). Exact distance between the two pegs was measured for its use in Equation 6. Channel depth at those locations, plus some extra places in between, were also measured to estimate the prevailing flow condition while remotely monitoring the study-stages on the provided web-based platform. Similarly, the distance between the top of the peg and the channel bottom was determined, creating a reference for the monitoring of the water surface (and associated water depth) associated with each trace and consequent use in Equation 2.

Between 3 ml (low flows) and 20 ml (high flows) of neat Rhodamine WT 20% were used. This dosage was to ensure both a "visual referencing" of the mixing process in the upper-mid portion of the study-reaches and a suitable end-concentration above background fluorescence (Figure 7a). The SCUFFA's minimum detection level is 0,04 ppb Rhodamine WT active ingredient and the sampling rate was set to 10 sec.

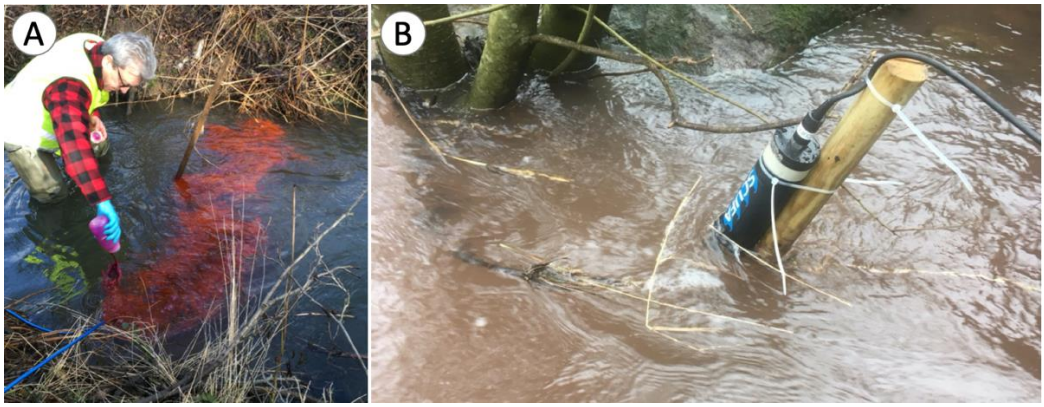

Figure 7 Rapid-deployment of a conservative-trace: A) Rhodamine WT instant injection at the upstream-end of the study site; and B) SCUFA [Self-Contained Underwater Fluorescence Apparatus] secured at the downstream-end. The SCUFFA's minimum detection level is 0,04 ppb Rhodamine WT active ingredient and the sampling rate was set to 10 sec. Photos: EA International (February 2019).

Every time a forecasted rain event was deemed sufficient to generate the desired flow condition, which was confirmed through remote-monitoring of the prevailing hydrograph, the rapid-deployment for a trace was triggered (*ca.* 1-hour travel time to the study-sites). The timing of the trace aimed to cover either the peak of the hydrograph or a base-flow condition, where flow fluctuation is minimal (Figure 8).

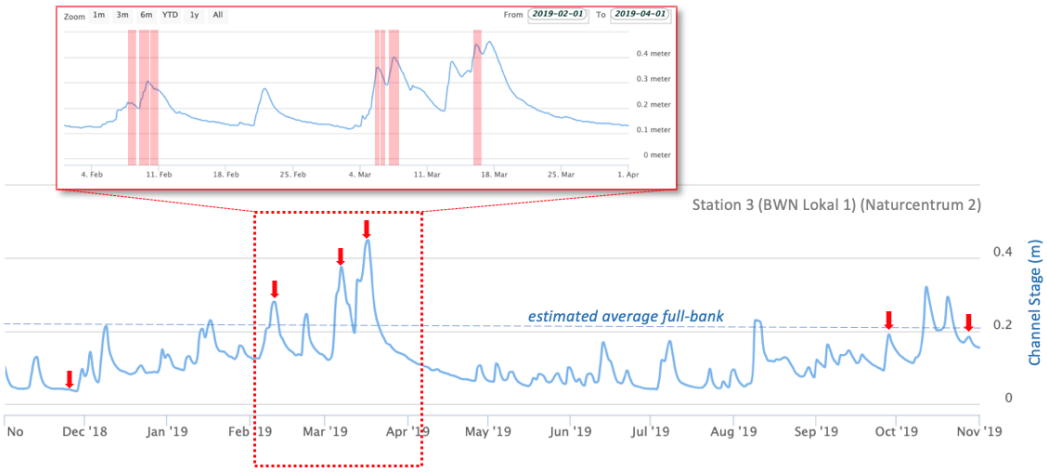

Figure 8 Timing of the 9 trace-sessions (9 traces x 4 sites = 36 traces) shown on the remote-monitoring hydrograph of Station 3 (Naturcentrum 2; Building With Nature local no. 1). Red arrows and columns indicate the trace-sessions.

4.4 Conservative-tracing – delivered results

A total of 39 traces were performed and analysed, with only one not providing reliable results due to sensor or equipment failure (obstruction of the sensor by plant material). These were executed during nine rain events and one at baseflow, just before a rain event (Figure 8). Consequently, one trace corresponded with a very low flow condition, two were around full-bank condition and seven were during overbank flow [a total of 16 traces, 4 flow conditions at 4 locations, was initially planned]. An example of results obtained from the analysis of breakthrough curves is shown in Figure 9. A summary of all the traces outcome is available in Annex 1.

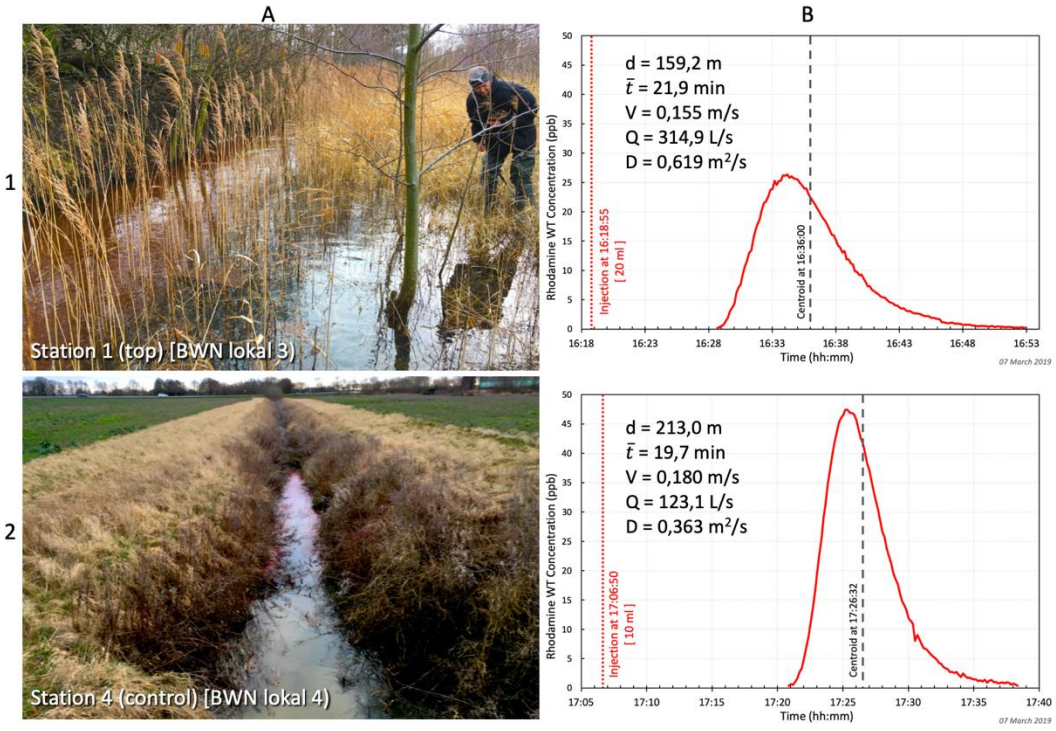

Figure 9 Example of results obtained from a set of traces performed at high flow. A) picture of the moving dye in a two-stage and rectified channels; and b) outcome of the analysis of the breakthrough curves. Photos: EA International (March 2019).

4.4.1 Trace-derived flow-rate (Q)

Data points have been derived from equations 4 and 4b (Figure 10). At the exception of Site 2, all data sets were used as input to the calibration process.

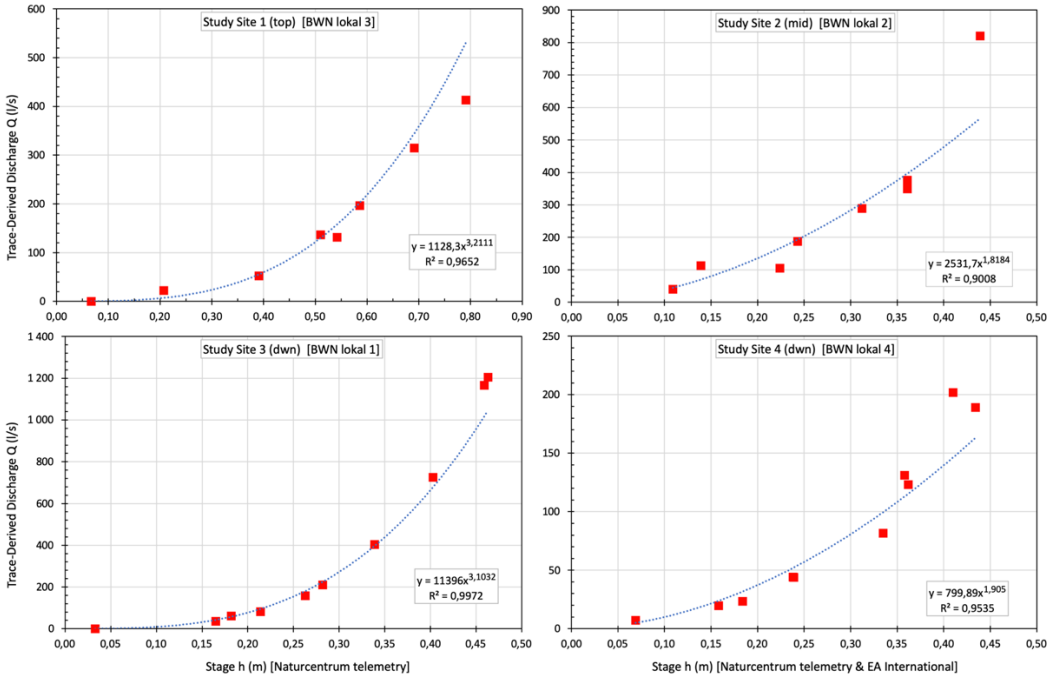

Figure 10 Trace-derived flow-rate as a function of recorded channel stage for the 4 study-sites.

4.4.2 Trace-derived average cross-sectional velocity ($\bar{V}$) and transit time ($\bar{t}$)

Results have been derived from equations 5 ($\bar{V}$) and 6 ($\bar{t}$) (Figure 11). At the exception of Site 2, the entire data set was used in the calibration process.

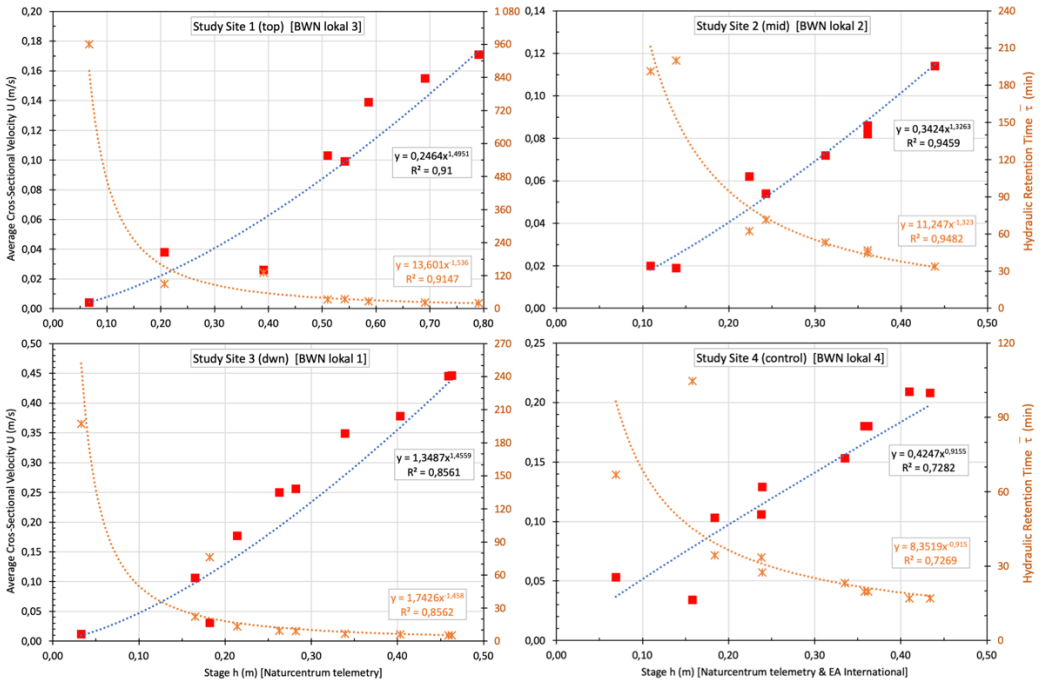

Figure 11 Trace-derived average cross-sectional velocity and hydraulic retention time as a function of recorded channel stage for the 4 study-sites.

4.4.3 Trace-derived Dispersion Coefficient (D)

Results derived from equations 7 and 8 (Figure 12) were compared to the hydrological model. It was however decided not to include them in the calibration process at this time.

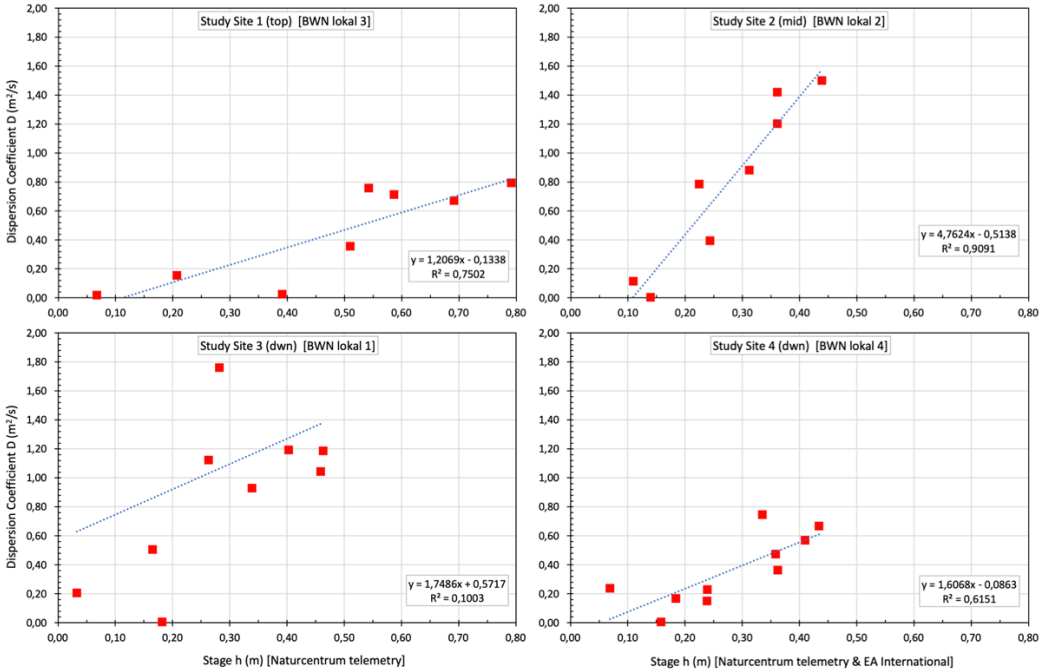

Figure 12 Trace-derived dispersion coefficient as a function of recorded channel stage.

4.5 Flow Rating Curve – stage-discharge relationship

As the discharge-stage rating curves were central to the calibration-validation process, the field flow-rates provided by Naturcentrum [tasked to developed the rating curves] were supplemented by 40 field-assessed and 38 trace-derived flows (Figure 13 and 14).

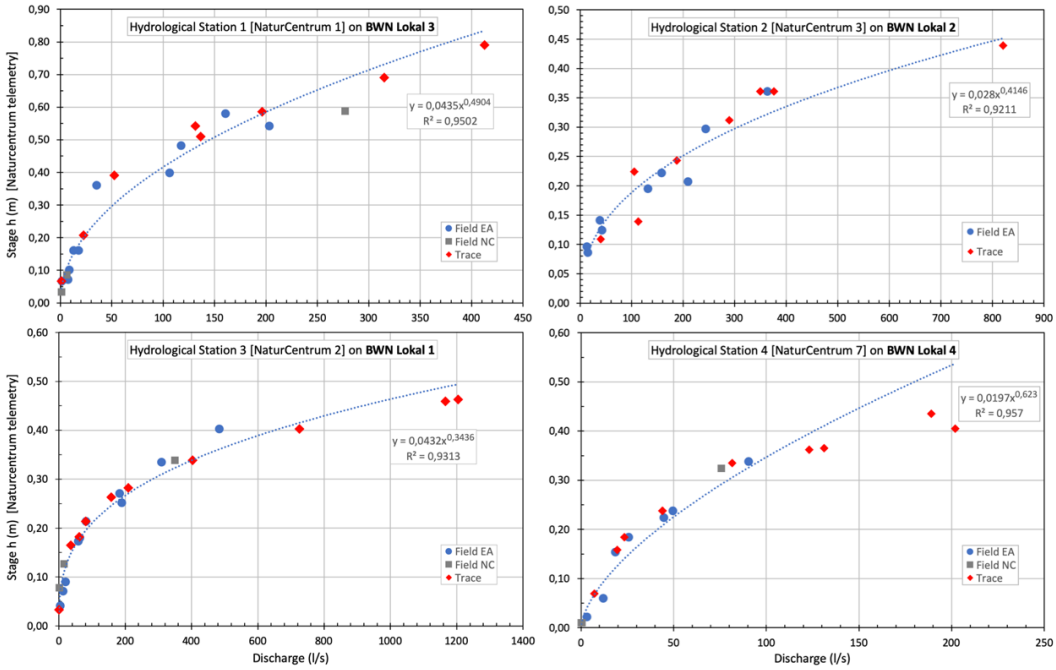

Figure 13 Final version of the stage-discharge relationship based on 3 sets of data.

Since Site 4 (control site) was equipped with a data logger on 25th February 2019 and that reliable recording started on 8th March 2018, only 4 of the 11 traces overlapped with the recorded hydrograph. The missing data had therefore to be estimated from manually recorded water depths (during traces and field-Q assessment activities) and a correlation between 1 and 3 stage recordings for specific rain/flow events. These estimated stage values are highlighted by a grey cell in the outcome summary table presented in Annex 2.

At the exception of Site 2 where the sediment-filled channel generated an almost permanent over-bank condition, the combined data set was used to identified a bank-full depth (stage) where the discharge-stage relationship changes (Figure 14). These bank-full values correlated well with field observations.

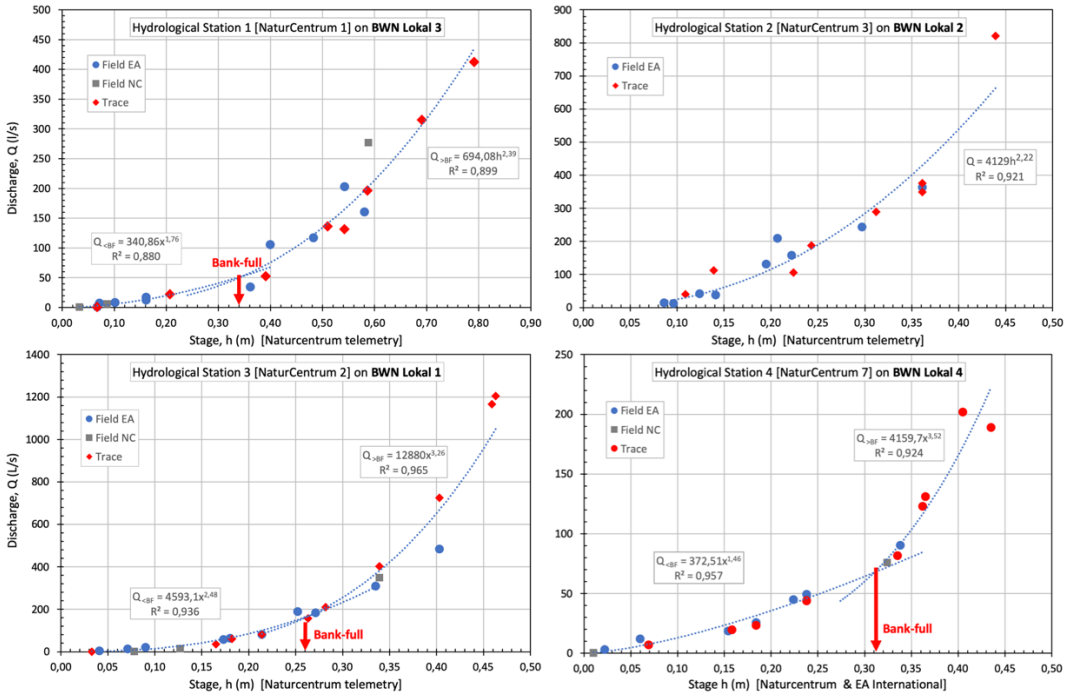

Figure 14 Study-sites rating curves showing an estimate of bank-full stage, where the discharge-stage relationship changes from an in-channel to an in-channel and over-bank condition.

4.6 Trace-Derived Manning Roughness Coefficient

A more precise assessment of both channel cross-sectional area and hydraulic radius (equation 1 and 1b) was needed to generate the composite channel cross-section used in computing the trace-derived Manning roughness coefficients (through equation 2), which were then used for a scale comparison with those producing the best fit during the hydrological model calibration process.

4.6.1 Complementary channel survey and resulting composite cross-sections

A high-resolution survey of the 4 study sites cross-sections (4 per sites) were conducted on 26th & 29th November 2019, when trees had lost most of their leaves. Location of these transects, as well as the one performed by Naturcentrum on 7th November 2019, is shown in figure 15.

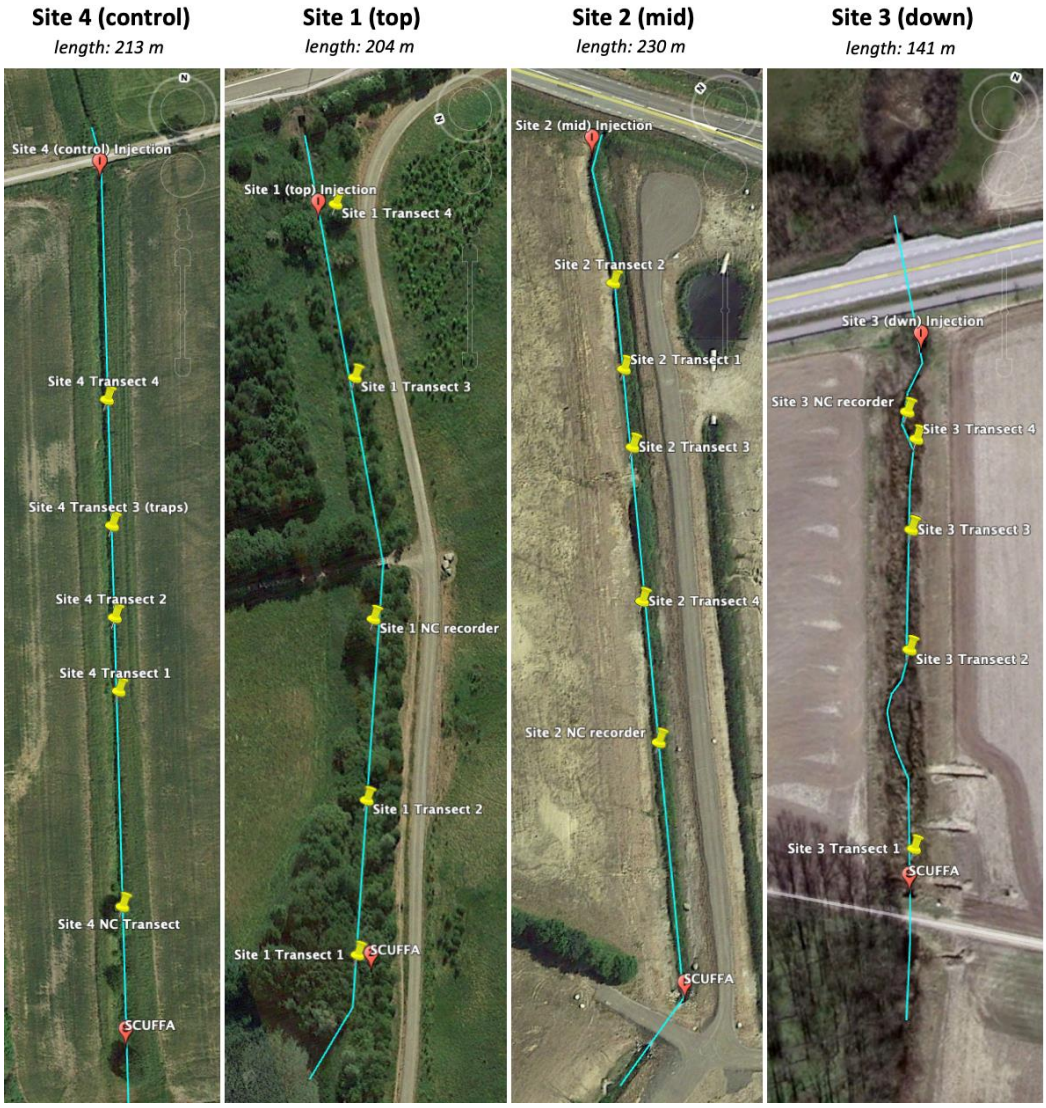

Figure 15 Relative length of the study sites showing the location of the trace injection and SCUFFA sites, as well as the locations of the cross-section high-resolution survey (Images from Google Earth, eye altitude ca. 335m).

The composite cross-section of each study was done manually, by first deriving new x (horizontal mark) and z (depth) coordinates from each of the individual transects. This was done by measuring "z" on a printed transect at specific horizontal distances standardised by measuring them from the centre of the channel bottom. These new values were then used to produce the composite cross-section profile on which the water depths associated with each trace were also plotted (Figure 16). Channel cross-sectional area (A), wetted perimeter (P) and consequently the hydraulic radius (R) were computed for each trace. Minimum and maximum cross-section profiles were also computed by assessing them from each standardised horizontal mark, but provided for comparison only at this stage of the study. A summary of the detailed field survey data is provided in Annex 3 while the resulting composite profiles are presented in Annex 4.

As Site 2's channel is sediment-filled with an almost permanent over-bank condition, and since it was not included in the modelling activities, a composite profile was not generated for this site at this time.

Individual cross-sections (column A) of Site 1 and 3 were also used to update the hydrological model as part of the calibration process focused on two-stage channel.

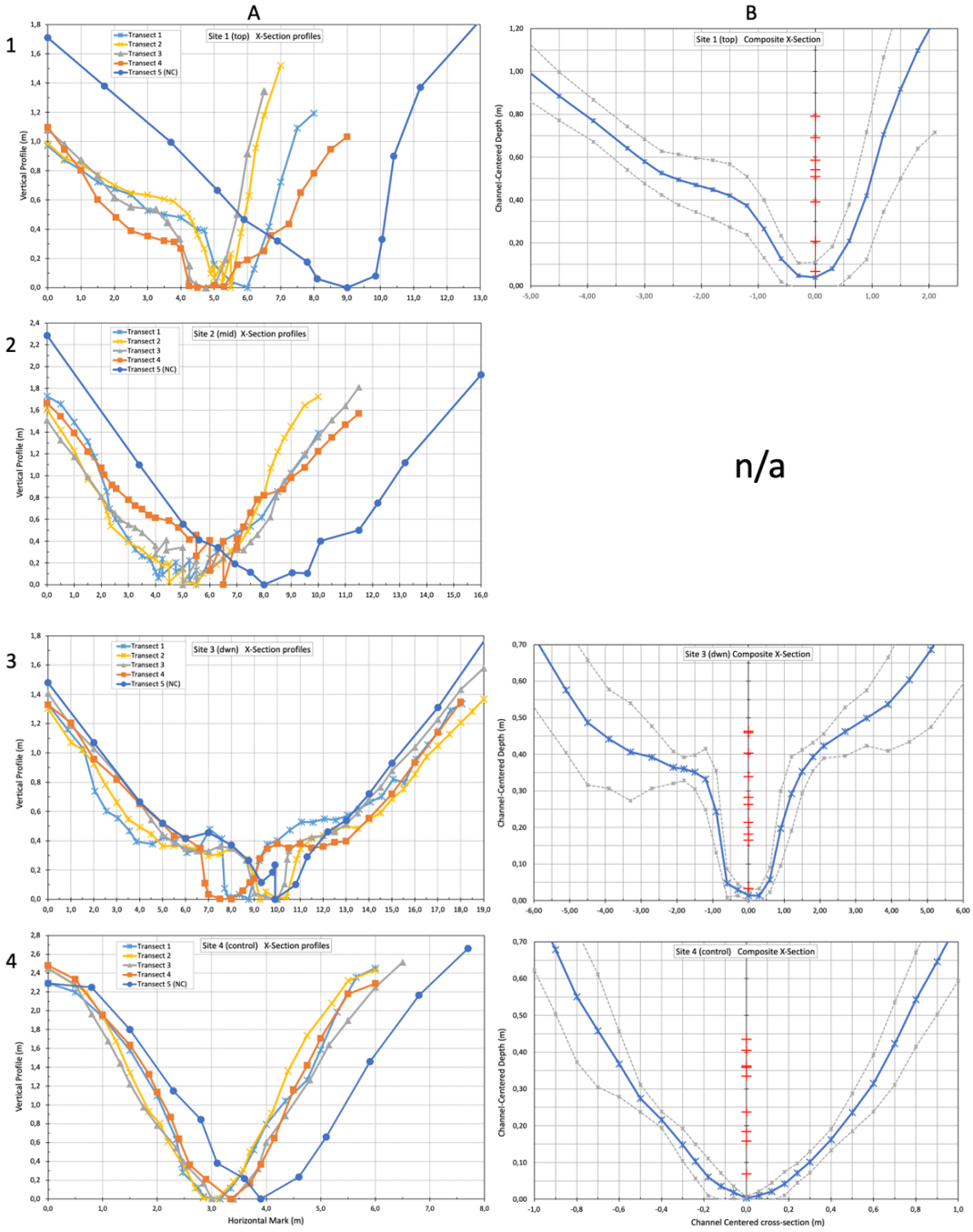

Figure 16 Individual (column A) and associated composite (column B) cross-sections of the two-stage channels (rows 1 to 3) and the traditional trapezoidal channel (row 4).

4.6.2 Resulting trace-derived Manning n

Using the composite channel cross-section developed for each site to assess a cross-section (A) associated with the prevailing recorded water depth (h), which is then used to compute the related wetted perimeter (P) and hydraulic radius (R), the Manning roughness coefficient associated with each trace is derived from equation 2. Although prevailing water slope is usually used, at this stage of the project, the overall channel bed-slope provided through the supplied 2018 survey was used as a surrogate value. These site bed-slopes are therefore the same as those used in the hydrological model. Values of Individual parameters used to derive Manning roughness at each site are provided in Annex 5.

Table 1 Summary of the trace-derived Manning roughness *n* for 2 two-stage channel site (Site 1 and 3) and the trapezoidal reference site (Site 4). The value of Manning roughness M (1/n) is also provided for ease of comparison with the Swedish literature.

Time Stamp	Site	Q	h	*n*	M
2018-11-28 03:20	1 (top)	1,10	0,067	1,012	0,99
2019-09-30 16:30	1 (top)	22,4	0,207	0,221	4,53
2019-10-28 14:20	1 (top)	52,4	0,391	0,439	2,28
2019-02-10 10:27	1 (top)	136,33	0,510	0,118	8,46
2019-02-09 16:12	1 (top)	131,39	0,542	0,129	7,75
2019-03-08 10:48	1 (top)	196,28	0,586	0,098	10,21
2019-03-07 16:40	1 (top)	314,94	0,691	0,100	10,03
2019-03-17 10:20	1 (top)	412,63	0,791	0,099	10,06
2018-11-27 13:19	3 (dwn)	*0,33*	*0,033*	0,310	3,23
2019-09-30 14:02	3 (dwn)	35,4	0,165	0,149	6,72
2019-10-28 12:11	3 (dwn)	60,9	0,182	0,128	7,83
2019-02-08 12:22	3 (dwn)	81,08	0,214	0,105	9,57
2019-02-09 14:01	3 (dwn)	157,5	0,263	0,083	12,12
2019-02-10 09:19	3 (dwn)	209,6	0,282	0,082	12,12
2019-03-08 11:01	3 (dwn)	403,10	0,339	0,064	15,71
2019-03-07 13:22	3 (dwn)	725,17	0,403	0,051	19,69
2019-03-17 12:30	3 (dwn)	1 165,84	0,459	0,045	22,16
2019-03-17 10:46	3 (dwn)	1 204,16	0,463	0,045	22,07
2018-11-27 20:15	4 (ref)	0,1	n/a		
2019-09-30 14:23	4 (ref)	7,1	0,069	0,137	7,32
2019-10-28 12:17	4 (ref)	19,6	0,158	0,367	2,73
2019-02-08 11:28	4 (ref)	23,43	0,184	0,133	7,52
2019-02-09 13:19	4 (ref)	43,89	0,238	0,123	8,13
2019-02-10 09:32	4 (ref)	44,1	0,238	0,150	6,68
2019-03-08 11:35	4 (ref)	81,62	0,335	0,128	7,83
2019-03-07 12:17	4 (ref)	131,13	*0,358*	0,114	8,80
2019-03-07 17:26	4 (ref)	123,10	*0,362*	0,113	8,81
2019-03-17 11:15	4 (ref)	202,0	0,405	0,105	9,49
2019-03-17 12:48	4 (ref)	189,1	0,435	0,111	9,05

The effect of in-channel plant die-out, the condition most likely to provide rapidly increasing resistance to flow, was explored by performing a trace right at the beginning of the plant

senescence (*i.e.*, end of the vegetative season; end of September) and at its highest point (end of October). At the exception of Site 3 which does not harbour in-channel vegetation, a strong effect of plant die-out on Manning roughness can be observed (Figure 17).

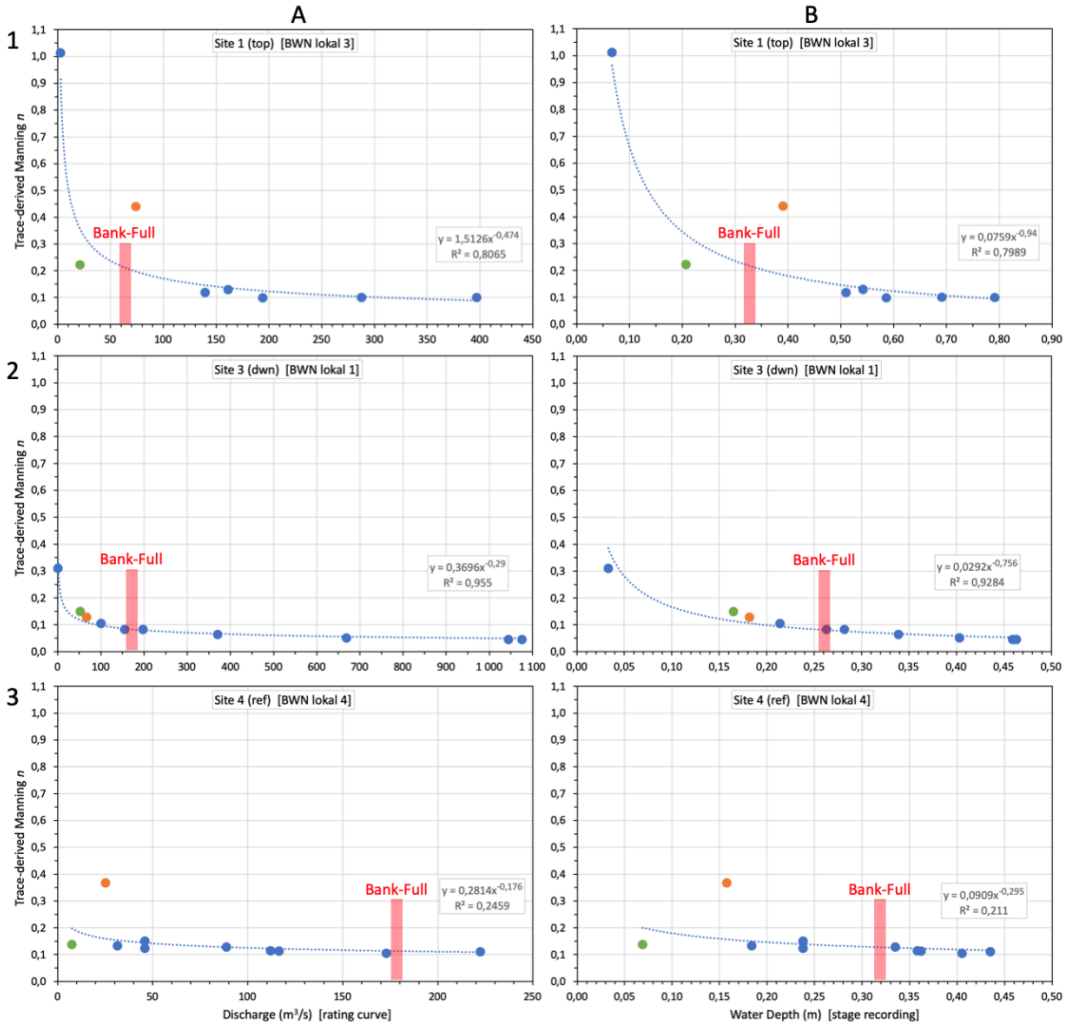

Figure 17 Relative changes in trace-derived Manning roughness *n* as a function of A) discharge [rating-curve derived], and B) water depth [stage recording], for 1 & 2) two stage-channel sites 1 and 3, and 3) the reference trapezoidal one. Bank-full condition derived from rating-curved are shown. The green point indicates a trace done at the beginning of the plant die-out (end of September 2019) and the orange one at its highest (end of October 2019).

It is important to remember that **trace-derived Manning roughness coefficients represent an "integrated" value of all flow resistance encountered over the entire reach studied**. This means that, under over-bank flow conditions, a trace-derived Manning n represents an average of the different roughness associated with the channel and the floodplains flows individually set in a hydrological model.

Although higher than those provided in literature reference-tables for natural streams and man-made channels (and therefore those of all hydrological modelling), the relationship between trace-derived Manning roughness coefficient and the prevailing discharge or water depth is in line with theoretical expectation (Figure 17). **The trace-derived values of *n* are therefore believed to be representative of the prevailing situation, as they are furthermore in the same range as those set in the hydrological model to obtain a suitable fit between discharge and water depth** (Figures 19 to 21).

5 Technical report on modelling activities [DHI Sverige AB]

5.1 Methodology

In order to provide a qualitative evaluation of the effect of a two-stage ditch on velocity reduction and retention times a 1D hydraulic model describing the Lussebäcken watercourse was established. The Lussebäcken basin and watercourse are described in Mike Urban CS. The model has been obtained from NSVA and was originally set up in 2008 (DHI, 2008). The model describes runoff from different types of surfaces, as well as discharge and water levels in the watercourse.

The model was updated with water management measures implemented over the last decade along with the change in land use. Model changes carried out are based on obtained documentation and in consultation with the client. The previous traditional drainage ditches have been modified to resemble the features of a natural stream in form of a two-stage ditch, on a few locations along the watercourse. An evaluation of the hydraulic effects of the two-stage ditches have been carried out through a comparative analysis with the traditional agricultural trench.

At four sites along Lussebäcken detailed surveys have been conducted prior and parallel to the hydraulic modelling. Cross-sectional measurements, water level records, tracer tests and stage-discharge relations formed the basis of the model and simulations. In discussion with the client, focus for evaluation was set on two of the three study-sites with two-stage design together with the reference with the traditional trapezoidal design. In figure 1, the sites included in the analysis are shown.

5.2 Analysis of two-stage channels in Lussebäcken

5.2.1 Hydrological calibration

A hydrological calibration of the model was carried out during spring 2008. Over the decade a series of measures have been implemented in Lussebäcken along with an increased urbanization in the catchment. Consequently, an additional calibration was applied.

Data for calibration was obtained from the weather station Helsingborg A and SHYPE calculations (ARO 259). The time resolution of obtained data was quarterly precipitation values, hourly temperature values and monthly evaporation values.

At three sites in the northern branches of Lussebäcken water level data have been recorded continuously since October 2018, Figure 1. The model was calibrated using rating curves from each of the sites. The rating curves were produced by EA International based on dye tracing conducted on several occasions, Figure 10.

The resulting hydrograph is presented in Figure 18, together with the discharge from the rating curve. A good fit is obtained for the range of conditions during the studied time period. It should however be noted that the calibration period is limited to less than a year and the validation of the correlation at high flows are hard to evaluate.

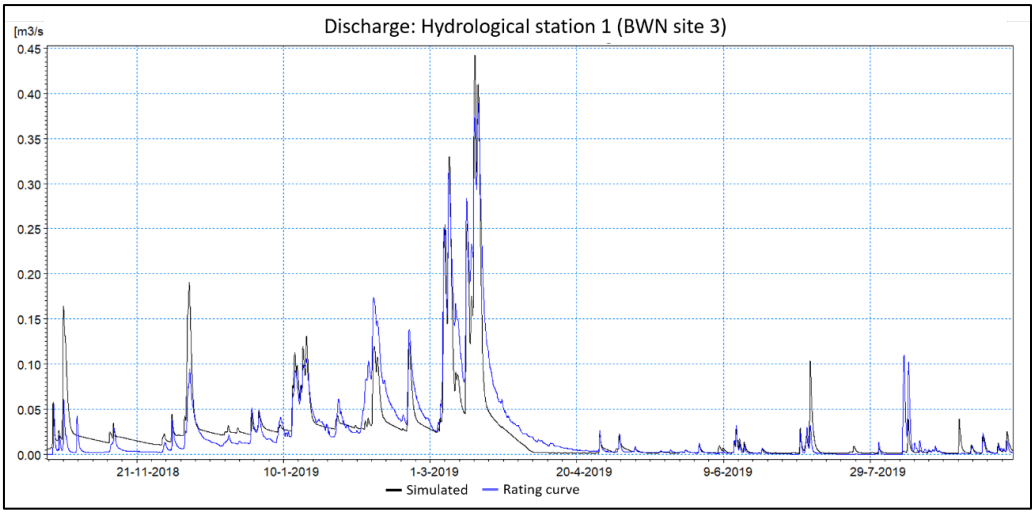

Figure 18 Discharge hydrograph at station 1, upstream the Långeberga industrial area. The discharge correlation between simulated and rating curve gives a R^2=0.84.

5.2.2 Hydraulic calibration and validation

5.2.2.1 Calibration

Calibration of the hydraulic model was conducted in order to produce accurate and credible results regarding water levels and velocities. Data used for calibration was recorded water level from data loggers. In order to exclude any uncertainties from the hydrological model the rating curve for each site was used to assign discharge at the studied sites. The parameter used for calibration is bed roughness. Typically, the low-flow channel has a lower roughness compared to the more vegetated benches. A differentiation in roughness between the main channel and adjoining benches was introduced in the model.

Cross-sectional measurements along with measurements for location, placement and size of culverts along the sections with two-stage ditches had been carried out by the municipality of Helsingborg. Additional cross-sectional measurements were provided by EA International with an improved resolution of the cross-sectional transects at the sites of hydrological station 1 and 3, Figure 16.

In Figures 19 to 21, the results of the calibration are presented for each of the sites. The water level is plotted with time. Included in the graphs are also calibrated bed roughness presented as Manning's n on a general cross-section of the site. The bed roughness represents an average resistance for the whole site. The objective with performed calibration is to reach as good results as possible but at the same time stay within reasonable values of Manning's n. Typically the bed roughness in a natural channel would be somewhere between n=0,2 to about n=0,03. Moreover, the roughness in the main channel will be lower than at the vegetated full bank benches.

At station 1 a good fit is obtained for the whole range of conditions during the studied time period, for station 3 an incredibly good fit is obtained for low flows and water depths to about 0.3 m. The results at the reference show a larger difference between simulated and observed depths but the trends and feedback are well captured in the model. At the reference the recorded water level series were measured during a shorter period.

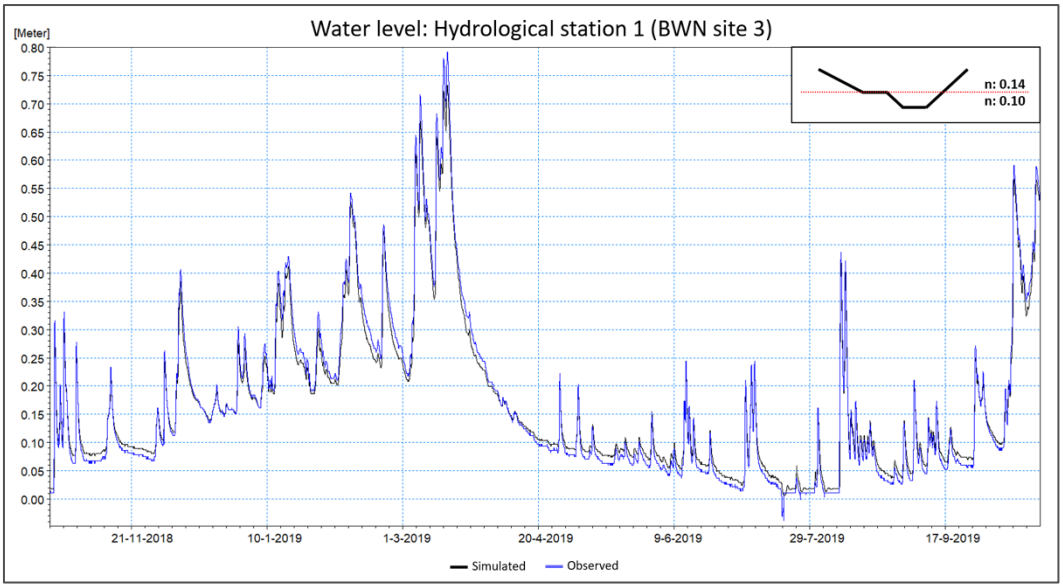

Figure 19 Simulated and observed water depth at Hydrological station 1. Presented is also a general cross-section at the and calibrated bed roughness (Manning's n).

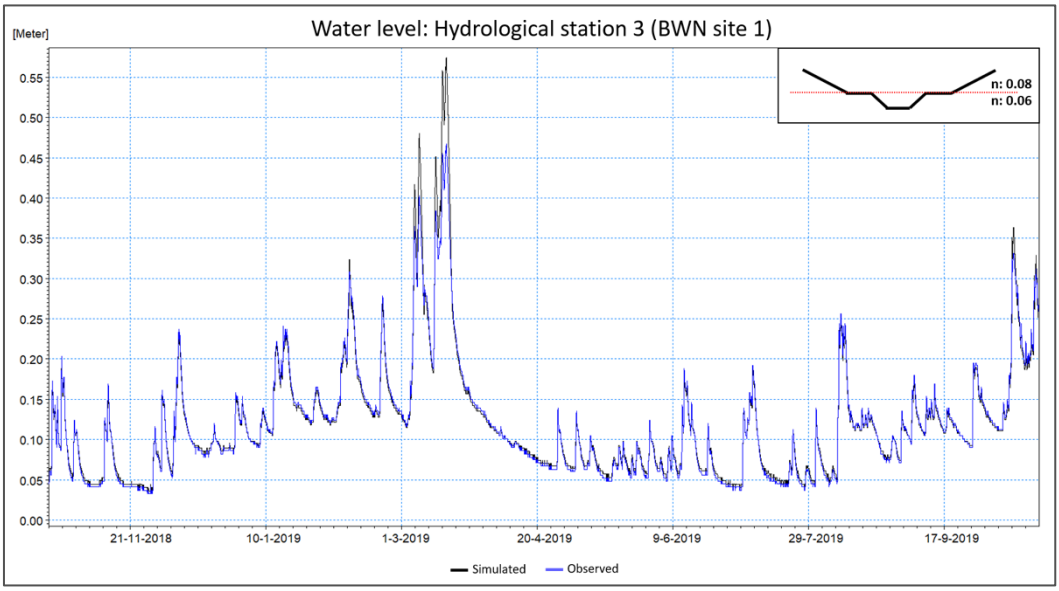

Figure 20 Simulated and observed water depth at Hydrological station 3. Presented is also a general cross-section at the and calibrated bed roughness (Manning's n).

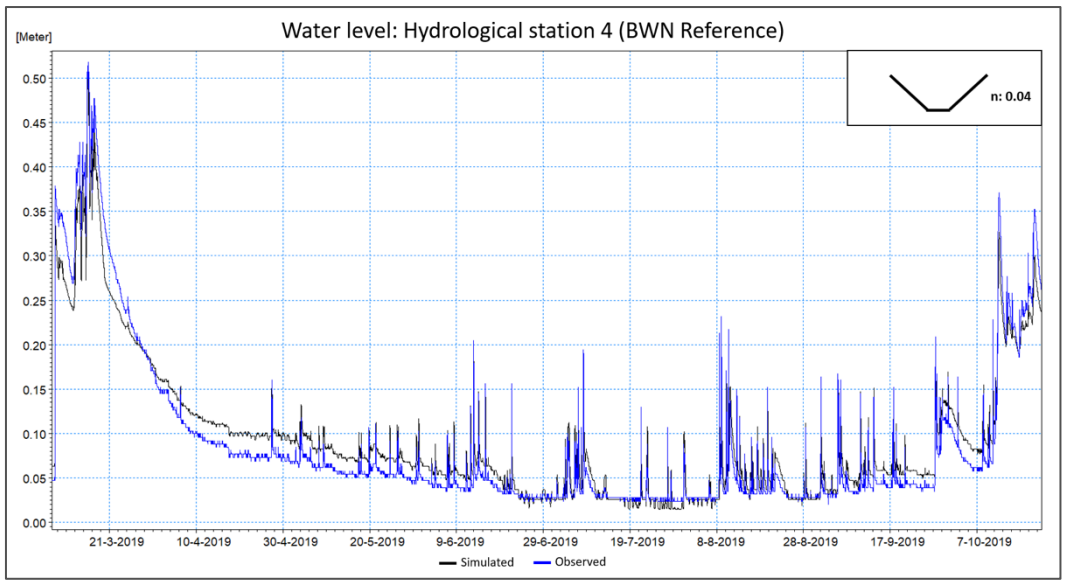

Figure 21 Simulated and observed water depth at Hydrological station 4. Presented is also a general cross-section at the and calibrated bed roughness (Manning's n).

5.2.2.2 Validation

To validate the model the average water velocity was computed and compared with the results of the tracer test performed at the sites of hydrological station 1 and 3.

The performed tracer test done in the field was replicated in the model. A tracer compound was added the Lussebäcken water course at a specific location for a given timestamp and the concentration over time measured at a location further downstream. The same injection and sample points where used in the model, as during the field assessment. The discharge is based on the rating-curve for the site in the same way as during calibration. In Figures 22, the results from simulation and tracer tests are presented as the average velocity and water level as a function of the discharge.

Site 3 has the most independence from other form of hydrodynamic influence. The stream segment has a distinct bed slope and lack backwater effect from downstream structures. Additionally, the greatest number of tracer tests used for validation have been conducted at the site.

The validation for site 3 gives a concurrent outcome with the calibration. The model has a good correlation with results from the tracer test. The best fit at site 3 is achieved at lower discharge, tendency at high discharge where the depths tend to get overestimated. Consequently, calculated average velocities have a similar deviation at higher discharge. Measured average velocities and modelled ones obtain a good fit up to about 200 l/s, for higher discharge the average velocity from the model are lower than observed during tracer tests. At site 1 the number of tracer tests carried out are less in number and the average velocities are much lower compared to site 3. Due to the low number of tests it is harder to draw a clear conclusion regarding the results. However, the same behaviour as for site 3 can be noticed where an overestimation in depth results in an underestimated velocity and vice-versa.

The calibration data cover a period of about one year. The number of events with high discharge during a year are very few and thereby the uncertainty in the water level response at these events large. In order to improve the model a longer period of data collection is needed.

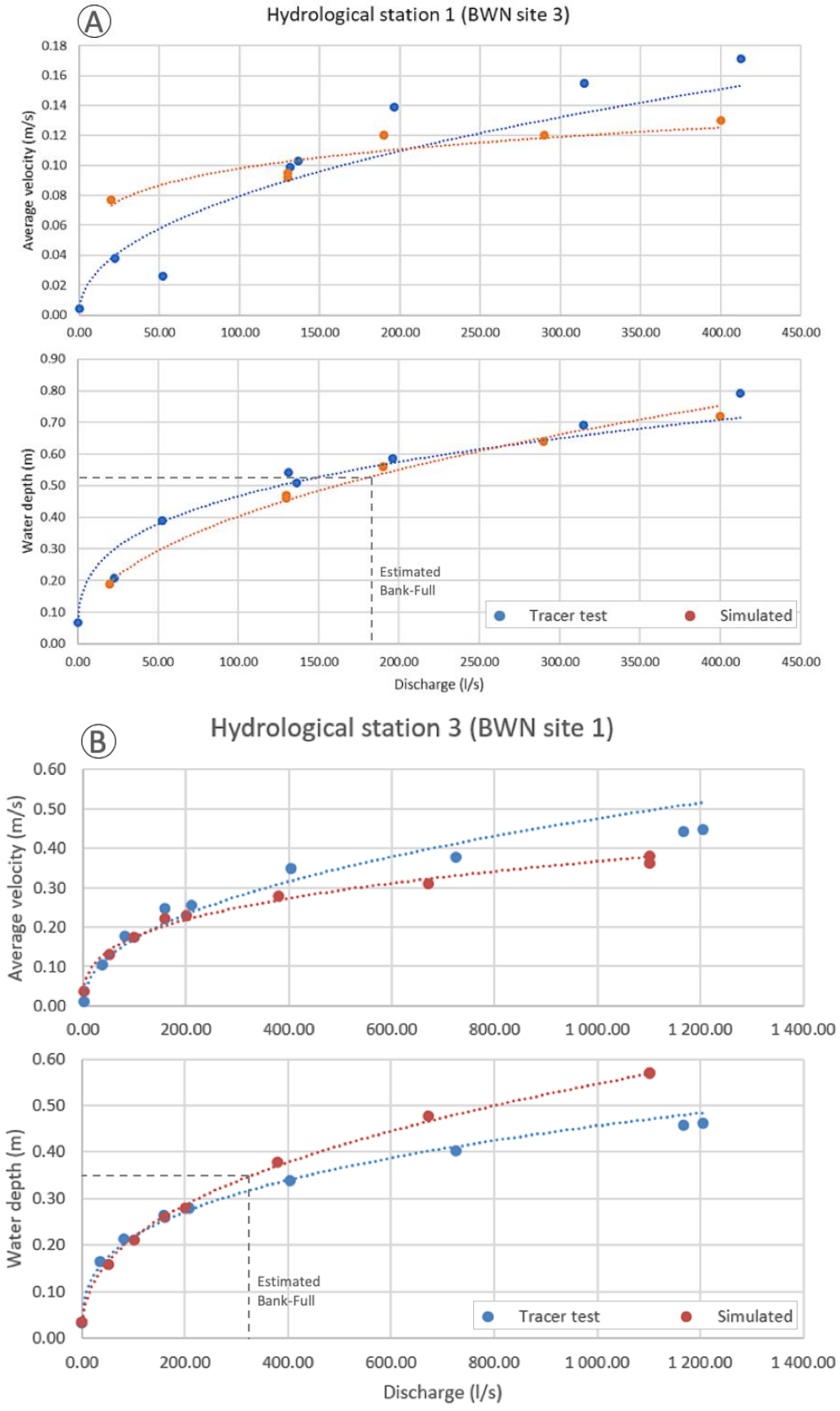

Figure 22 Graphs presenting results from simulation and tracer tests for sites 1 (A) and 3 (B). The results are presented in a scatter plot with data points together with a trendline. The average velocity is plotted as a function of discharge in the upper graph and water depth as a function of discharge in lower graph. Estimated Bank-Full discharge and associated water depth are also indicated.

5.2.3 Analysed scenarios

The main channel of the of a two-stage ditch and a trapezoidal ditch are similar. A more interesting dynamics of the two-stage ditch is at full bank when the benches are active, and the wet perimeter grow considerably. In a natural stream the full bank discharge has an approximately constant return period of 1.5 year. Consequently, the effect of the two-stage ditch was studied for the 1.5-year discharge.

The 1.5-year discharge was calculated for the hydrological stations 1 and 3 using a frequency analysis. The frequency analysis was based on modelled discharge for a simulation period of 25 years (1995 – 2019). The simulation period corresponds to the period the weather station Helsingborg A has been active and recorded precipitation values with 15 min resolution. Using Log-Pearson type 3 distribution the discharge with return period of 1.5 year at hydrological station 1 is calculated to 0.44 m^3/s and at hydrological station 3 to 0.63 m^3/s. The frequency period plot of the two sites are presented in Figure 23.

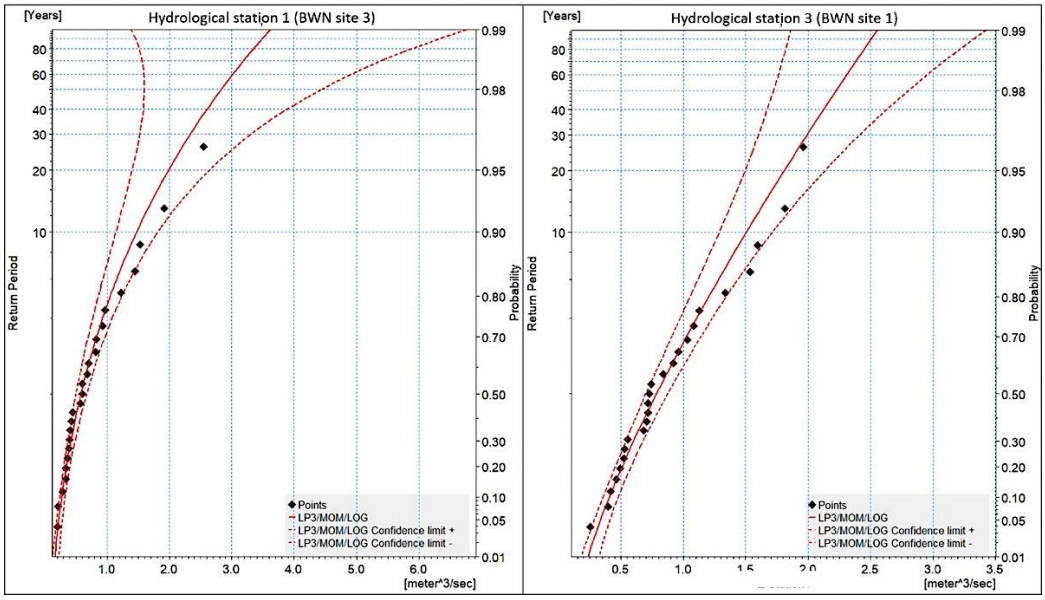

Figure 23 Frequency plot for hydrological station 1 and 3. From the result the return periods corresponding to specific discharge can be read.

5.2.4 Evaluation of the two-stage ditch

The 1.5-year discharge was added to the model as a boundary condition upstream the studied sites of hydrological station 1 and 3. The effect of the two-stage design was evaluated by comparing the results of the 1.5-year discharge with a scenario where the cross-section at hydrological station 1 and 3 are replaced with the design of the reference site (hydrological station 4). The cross-section of the agricultural trapezoidal ditch has a side slope of 1:1.5 and a bottom width of 0.3 m. The Manning's M correspond to n = 0,04. General cross-sections of both sites with two-stage ditches and the reference trapezoidal ditch are presented in Figure 24. On the greater part of the reach for the hydrological station 1 a bench is only present on one of the banks.

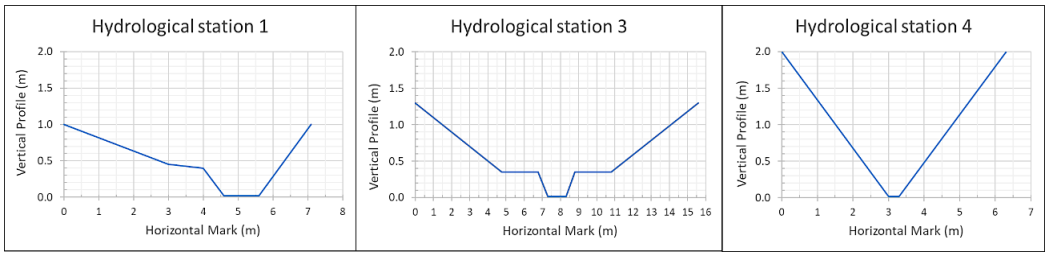

Figure 24 General cross-sections of the studied sites. An evaluation of the effect of two-stage ditches in Lussebäcken have been performed by comparing results when the trapezoidal ditch at hydrological station 4 has replaced the current stream design.

The results of the simulated scenarios are presented in Table 2. The results indicate that the two-stage channels decrease the average velocities and thereby increase the residence time considerably.

The calculated depth decreases at station 1 but increases at station 3 when replacing the current two-stage channel with the trapezoidal channel of station 4. The water depths at a given discharge are affected by downstream structures, bed slope, cross-sectional area and bed roughness. At site 1 the replacement by the trapezoidal ditch implies a smaller cross-sectional area but also a lower roughness, which combined results in a lower depth. At site 3 the cross-section areas are reduced considerably more, whereas the difference in bed roughness are lower, resulting in a higher depth.

Table 2 Results from simulation of a 1.5-year discharge ($Q_{1.5}$) at hydrological station 1 and 3. Presented are length of the site and computed depth, average velocity (U) and residence time (t).

Location	Design	$Q_{1.5y}$ (m^3/s)	Length (m)	Depth (m)	U (m/s)	t (min)
Hydrological station 1	Two-stage ditch	0.44	202	0.76	0.12	28.1
Hydrological station 1	Trapezoidal ditch	0.44	202	0.62	0.25	13.5
Hydrological station 3	Two-stage ditch	0.63	149	0.42	0.31	8.0
Hydrological station 3	Trapezoidal ditch	0.63	149	0.62	0.52	4.8

6 Joint analysis of two-stage channel hydraulic performance

The updated and calibrated model of Lussebäcken now captures reasonably well the overall hydraulic behaviour of the studied sites. Consequently, the "retrofitting" scenario – *i.e.*, applying the trapezoidal cross-section of Site 4 to the prevailing two-stage channels of Sites 1 and 3 – allows to infer the performance of a two-stage channel "restoration" scenario with regard to its effect on water velocity, water depth and, to a certain extent, discharge and flow peak.

The retrofitting scenario has been analysed in simulations of **1)** a full-bank discharge [$Q_{1.5}$], and **2)** the temporal discharge hydrograph established through the hydrological calibration process (section 5.2.1). As the trapezoidal geometry of Site 4 was seen as representative of the rectified drainage channels in the vicinity of the study sites, no scaling was used at this time when it was applied (Figure 25).

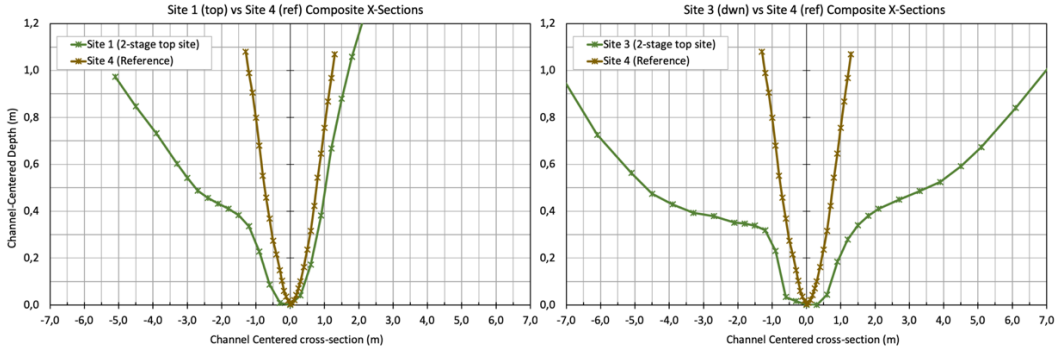

Figure 25 Comparative changes in composite channel geometry when the trapezoidal cross-section of Site 4 is applied to the prevailing ones.

6.1 Effect of two-stage channel geometry on full-bank flow ($Q_{1.5}$)

It can be inferred from the simulation, that restoring a trapezoidal drainage channel to a two-stage cross-sections similar to those in Lussebäcken could, on average, reduce the water depth associated with a $Q_{1.5}$ by about 5% (*ca.* 0,05 folds), the water velocity by 80% (*ca.* 0,8 folds) and increase the hydraulic residence time by 50% (*ca.* 0,5 folds) (Table 3).

Table 3 Inferred potential changes (∂ and %) in computed depth (D), average velocity (V) and residence time (t) associated with their respective $Q_{1.5}$ if Sites 1 and 3 had been trapezoidal ditches dimensioned like Site 4 before being restored to two-stage channels.

Location (length)	∂ D		∂ V		∂ t	
	(m)	%	(m/s)	%	(min)	%
Site 1 (202 m)	+0,18	+18%	-1,08	-108%	+0,52	+52%
Site 3 (149 m)	-0,48	-48%	-0,68	-68%	+0,40	+40%
Average change	***ca.* -5%**		***ca.* -80%**		***ca.* +50%**	

Note: the % change is a function of the original two-stage cross-section.

The counterintuitive increase in water depth observed after the "restoration" of Site 1 is due to **1)** the smaller gain in cross-section compared to Site 3 owing to the presence of only one floodplain (Figure 25); and, **2)** the large decrease in velocity associated with a significant increase in hydraulic roughness, from a Manning n of 0.04 of the almost bare drainage ditch to an average n of 0.12 associated with increased in-channel and floodplain vegetation. Consequently, it can safely be assumed that these changes would have been even more pronounced if a two-floodplain design was present at both sites.

Halving of the water velocity under full-bank condition therefore infers a significant decrease in both bank erosion and sediment transport potentials. This, in combination with a substantial increase in hydraulic retention time, further promote the potential of nutrient retention in the watershed as these effects remain under over-bank flow condition.

6.2 Effect of two-stage channel geometry on peak-flows

Outcomes based on simulated discharge hydrographs (Oct. 2018 to Nov. 2019) show that fitting a trapezoidal geometry to the two-stage channel of Sites 1 and 3 (respectively one- and two-floodplain designs) produced similar results; with an average increase in discharge of *ca.* 5% over the simulated 2018-2019 hydrological year (Figure 26).

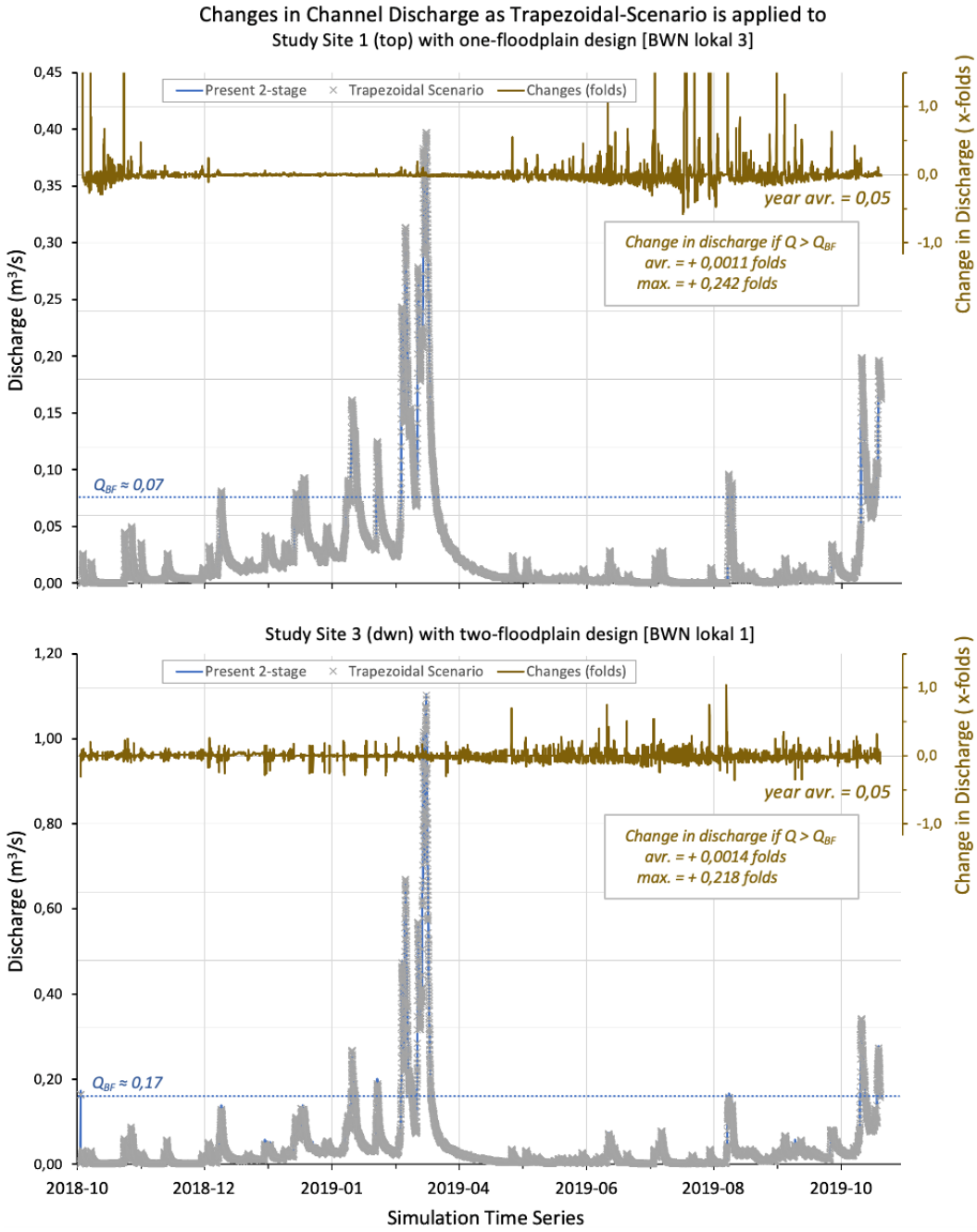

Figure 26 Changes in discharge when the trapezoidal geometry of Site 4 is applied to Sites1 and 3 two-stage channels. The hydrographs and magnitude of change (folds) over a one-year simulation are shown.

Most of the large positive increases in peak flow are associated with very low discharges due to a decrease in channel cross-section area, since the trapezoidal channel of Site 4 is narrower than those of Sites 1 and 3 (Figure 25). Consequently, if only overbank flow is considered (*i.e.*, $Q > Q_{FB}$; where full-bank is defined from site discharge rating curves, Figure 14), the average increase in overbank discharge is significantly lower (*ca.* 0,1%). Although only marginally different, the largest increase in overbank flow is observed at Site 3; which infers that a two-floodplain design has a slightly higher potential in reducing peak-flows.

Although area over the length of the Lussebäcken two-stage channel floodplains add static storage capacity (*i.e.*, depth of water if it was not moving), the effect on overbank flow remains marginal as demonstrated by the outcome of the scenario. **In accordance to the Manning equation, hydraulic roughness is a key element in increasing water depth under steady flow**; hence locally increasing the volume of water held over the floodplains.

Figure 27 Pictures of overbank flow showing that, although volumetric storage is significant over the floodplains, the majority of the flow (m^3/s) is in fact confined to the main channel as depicted by the path of the tracer compound some distance downstream of the injection site. Photos: EA International (February-March 2019).

One possible hindrance to a higher performance may therefore be linked to the fact that a large portion of the floodplain's "roughness" is actually not used. Field observations indicate that, although hydraulic storage is volumetrically significant during overbank conditions, the majority of the flow (m^3/s) is in fact confined to the main channel regardless of the flow depth. This was made clearly visible downstream of the injection point by the speed at which the main bulk of the Rhodamine WT was moving through the main channel

in comparison to the lateral exchange with the floodplains (Figure 27 and cover photo). At the exception of the trapezoidal reference channel (Site 4), this phenomenon was present at all overbank-flow traces. Consequently, the bulk of an overbank peak-flow (*i.e.*, fast moving volume) is therefore passing right through the main channel area without much of the attenuation that could have been provided by floodplains (*i.e.*, the wetted perimeter roughness).

Nevertheless, like designed stormwater ponds and wetlands, the most effective way to achieve peak-flow attenuation in managed running-water systems is through **extended detention**; where part of the stormwater is temporarily stored behind low-head obstructions spanning most of the floodplain width, to be released at a rate slightly lower than the one at which it entered. Although it would mean temporarily creating a large impoundment, the same result could also be achieved by restricting reach outflow (*i.e.*, by selecting a smaller diameter culvert pipe for example). Whilst the total volume of stormwater passing through would be unchanged, the rate at which it would flows through would be momentarily reduced; hence attenuating to some extent peek events.

This illustrates that, unless low-head structures (such as riffle-pools or small woody debris-dams) are in place to promote some type of impounding across the entire floodplain and along the entire reach, no significant flow attenuation can be achieved on relatively short restoration reaches.

Like any other running-water ecosystems, although two-stage channel drainage cannot provide "front-line" protection against high peak-flows, they are an integral part of the water conservation measures. As such, only a full-scale "restoration" scenario – where these cross-sections are applied to a significantly larger portion of the Lussebäcken drainage basin – can provide insight in the specific effect of a comprehensive two-stage channel approach on downstream flood-risk reduction.

6.3 Effect of two-stage channel geometry on water depth & velocity

Results based on the simulated hydrographs (Oct. 2018 to Nov. 2019) show that fitting a trapezoidal geometry to the two-stage cross-sections of Sites 1 and 3 produces a significant increase in water velocity and decrease in water depth; with the rate and final level of changes associated to each channel initial characteristics (Figures 28 and 29).

When the full flow-range is considered, the one-floodplain design demonstrates a -36% average decrease (*i.e.*, -0,36 folds) in water depth and an almost doubling in associated in water velocity (*i.e.,* +1,81 folds increase); whilst the two-stage channel design displays no significant change in water depth (*i.e.*, +0,03 folds) but an almost quadrupling in water velocity (*i.e.*, +3,89 folds average increase). However, if only overbank flow is considered (*i.e.*, $Q > Q_{FB}$), applying the characteristics of the trapezoidal control site to the one-floodplain site decreases water depth by an average of 26% and increases water velocity by 1,15 folds (Figure 28). In contrast, applying the same control site characteristics to the two-floodplains site generates a significant 35% average increase in water depth (*i.e.*, +0,35 folds) and an associated 1,62 folds average increase in water velocity (Figure 29).

Although some variation in behaviour can be attributed to the model having a better fit with the field trace-derived values for Site 3 (Figure 22), differences in site characteristics are the most likely driving factors. Whilst cross-section geometry (1 *vs.* 2 floodplains, hence the extent of the wetted perimeter) and reach bed-slope (0,10% and 0,45% at Site 1 and 3 respectively) do play an important role, in this particular simulation, the relative change in hydraulic roughness as the scenario is applied is key to the difference in response. In addition, a pond immediately downstream of Site 1 acts as a "hydraulic control" at higher flows, further explaining the difference in water depth changes during overbank condition.

The highly vegetated and silted channel of Site 1 was assigned a Manning roughness coefficient of n = 0,10 whilst the one for its singular floodplain was set to n = 0,14; which is respectively 2,5 and 3,5 folds larger that the n = 0,04 of the trapezoidal control Site 4. In

comparison, the sediment and vegetation free channel of Site 3 was set at n = 0,06 and its two floodplains to n = 0,08; which is respectively 1,5 and 2,0 folds larger that the n = 0,04 of the trapezoidal control Site 4. Furthermore, when assessed from the schematic cross-sections used in the hydrological model (Figure 24 and 30), the passive storage area associated with a 30 cm over-bank flow (maximum depth over the floodplains observed over 2019) is *ca.* 50 % smaller for Site 1 when compared to Site 3.

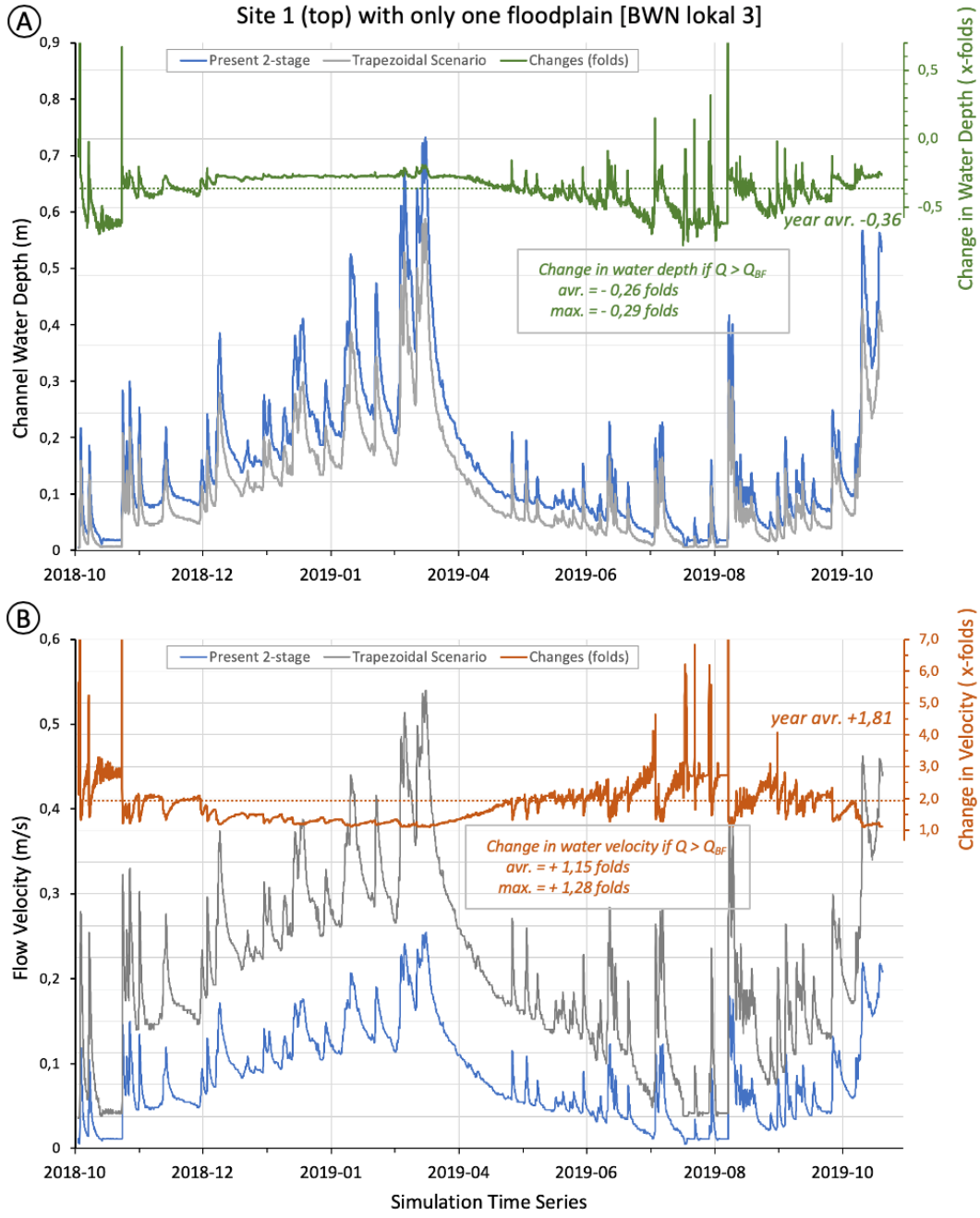

Figure 28 Temporal variation and magnitude of change following the "retrofit to trapezoidal drainage ditch" scenario on Site 1 one floodplain two-stage channel over a one-year simulation. A) water depth; B) water velocity. The magnitude of change is express in folds.

Because of its more established characteristics (*i.e.*, mature riparian trees providing shading, hence minimizing in-channel vegetation growth and sediment accumulation; more "stream-like" channel bottom demonstrating material consolidation with potential for riffle-pool structures) and the absence of downstream hydraulic control, the outcome of the scenario from Site 3 is seen as the most representative basis for assessing the

hydraulic effects of two-stage channel restorations. Nevertheless, the outcome of the scenario from Site 1 provides some insights on the joint impacts of higher hydraulic roughness (*i.e.*, in-channel and floodplain vegetation) and one-floodplain design approach.

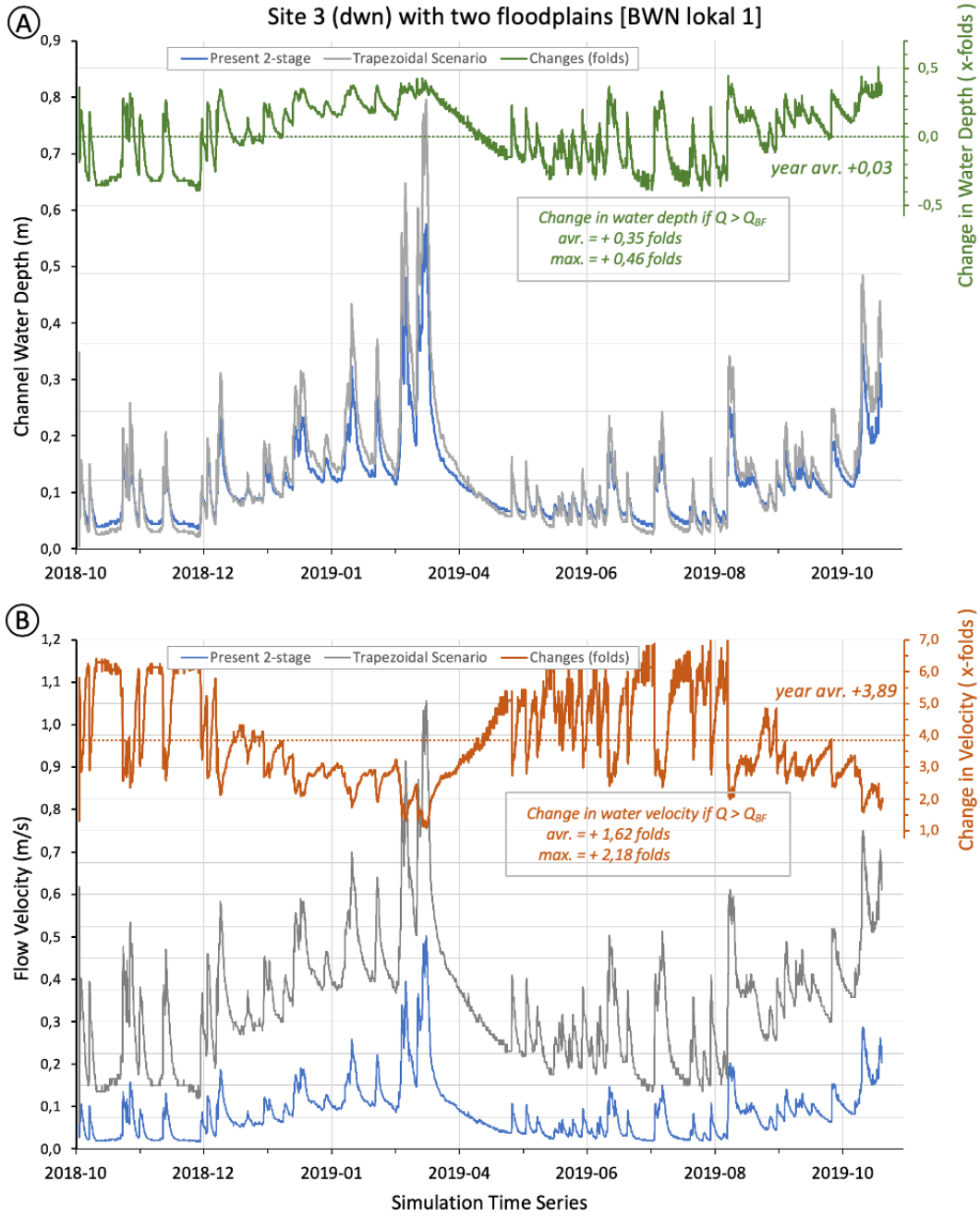

Figure 29 Temporal variation and magnitude of change following the "retrofit to trapezoidal drainage ditch" scenario on Site 3 two floodplains two-stage channel over a one-year simulation. A) water depth; B) water velocity. The magnitude of change is express in folds.

It can therefore be inferred that restoration of a trapezoidal drainage ditch based on either of the two-stage channel sites characteristics would significantly decrease water velocity **during overbank flows** (*i.e.*, $Q > Q_{bf}$) by a range average of -1,62 to -1,15 folds (respectively Sites 3 and 1), whilst water depth would be decreased by 35% based on Site 3 characteristics and increased by 26% based on Site 1 characteristics (Figure 31). The largest rate of changes is however observed at low discharge, within the confine of the main-channel. Whilst rate of changes in both water depth and velocity is more progressive under the Site 3 characteristics scenario, it is more pronounced in Site 1

scenario due to the joint influence of high hydraulic roughness and shallow bed-slope.

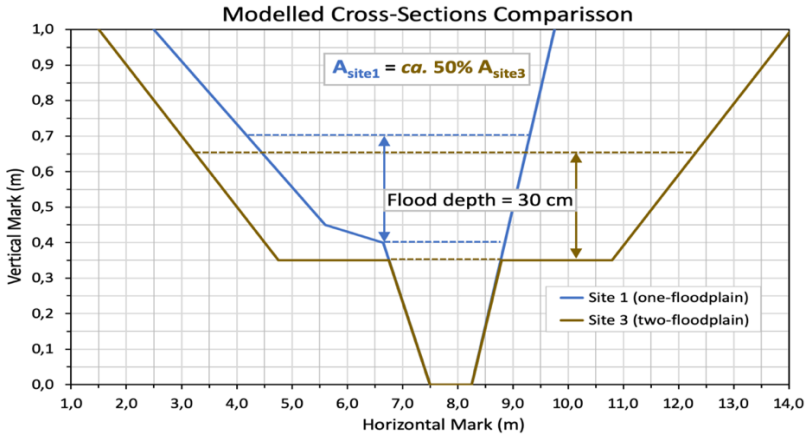

Figure 30 Schematic cross-sections of Sites 1 and 3 used in the hydrological model. Difference in passive water storage area associated with a 30 cm over-bank flow is shown.

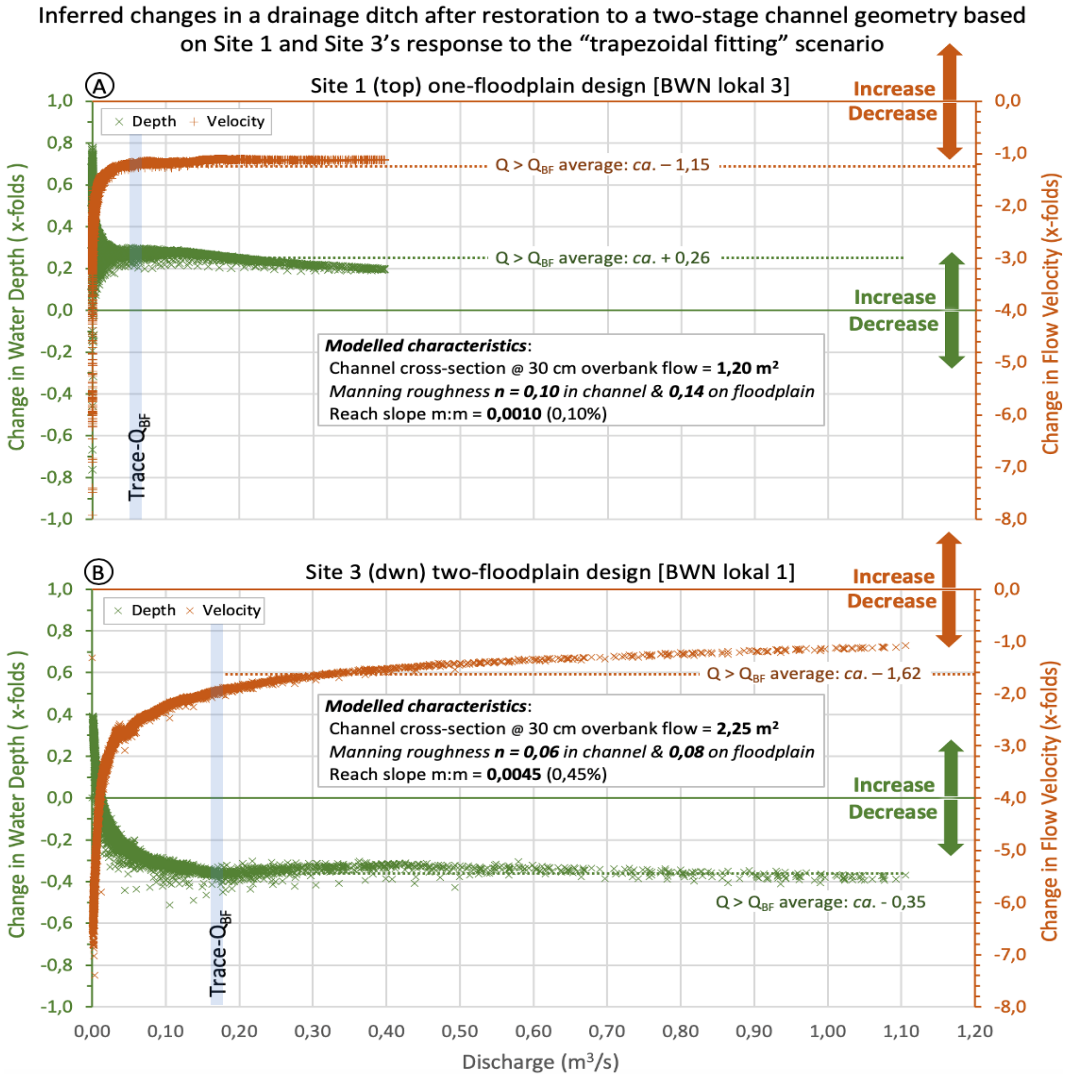

Figure 31 Inferred changes in water depth and velocity following restoration of a trapezoidal drainage ditch based on Site 1 (A) and 3 (B) characteristics. Magnitude of change (folds) are presented as a function of the respective discharge modelled for the two-stage channels. Respective trace-derived full-bank discharge are indicated.

The synergetic effect of high hydraulic roughness and shallow bed-slope, compounded by rising level of hydrological control exerted by the downstream pond, are behind the final *ca.* 26% increase in water depth when compared to what would have been observed in the unrestored trapezoidal drainage ditch. However, considering that Site 3 scenario is more representative of a "natural stream" restoration state, the one-floodplain design would have generated a lower increase or even a slight decrease in water depth if a lower hydraulic roughness was applied (*i.e.*, less dense in-channel and floodplain vegetation) and if no significant downstream hydraulic control was present.

The simulations clearly indicate that restoration of a trapezoidal drainage ditch to a two-floodplain two-stage channel cross-section can significantly reduce both water depth and velocity compared to what it would have been if the restoration was not performed (Figure 32). It also infers that, whilst a significant reduction in water velocity would reduce risks of channel and bank erosion (*i.e.*, sediment transport), reduction in water depth would help minimize the impact of high channel flows on the efficiency of underground drainage system (*i.e.*, "back-flow" effect in drainage pipes).

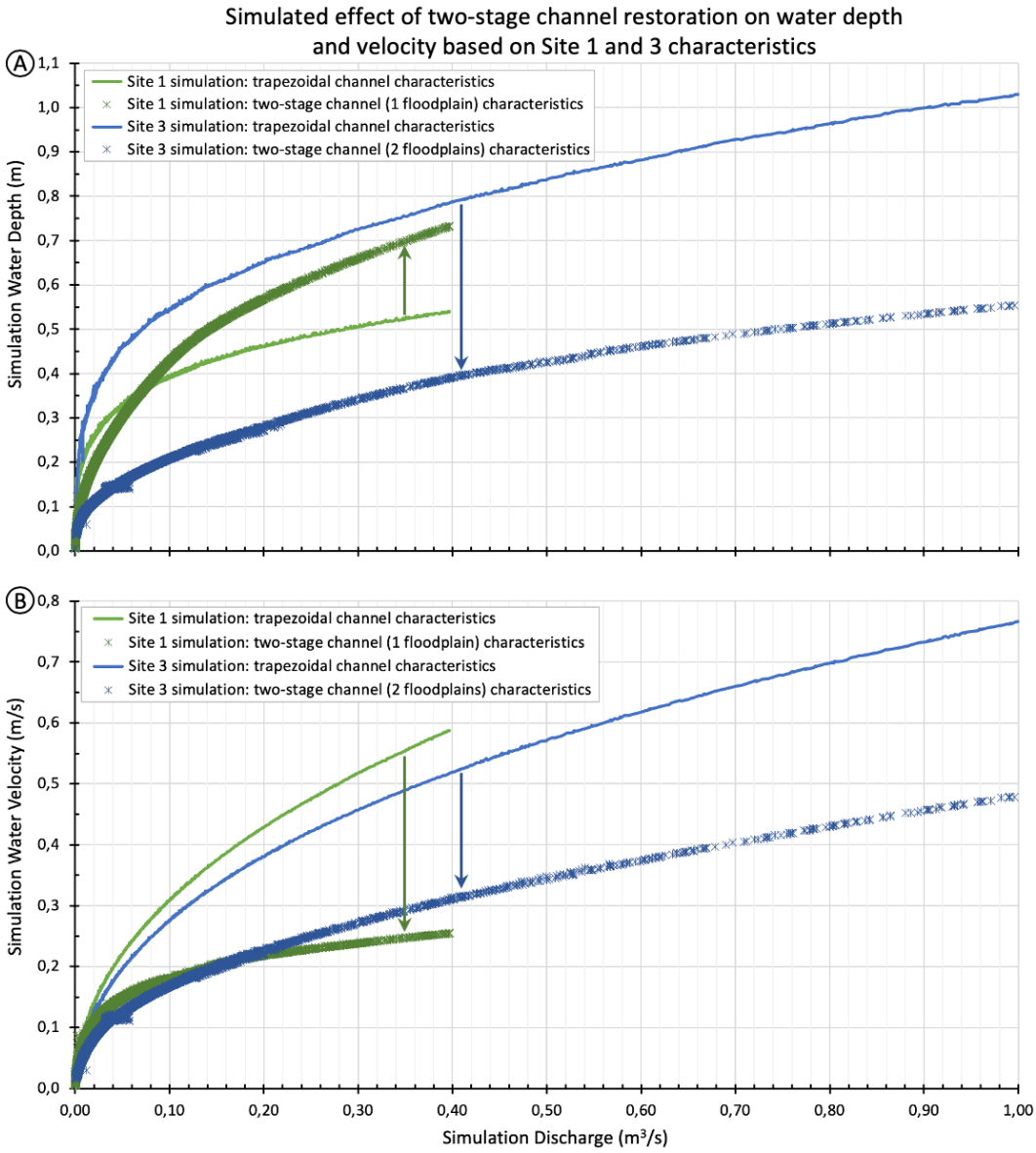

Figure 32 Simulated effect of two-stage channel restoration on water depth (A) and water velocity (B) as discharge increase based on Site 1 and Site 3 characteristics.

The simulation also highlights the importance of controlling in-channel vegetation (*i.e.*, hydraulic roughness) if the reach to be restored with a shallow slope. Most importantly, it also clearly shows that, under shallow bed-slope, water depth reduction performance will be less if a downstream pond is present (*i.e.*, downstream hydraulic control).

Anticipated differences in water depth and velocity associated with a restoration based on Sites 1 and 3 characteristics can also be visualized by applying the "modelled changes" to actual high and low flow events that have respectively occurred on 30th September and 7th March 2019 (Figure 33). Water depth, velocity and discharge in the two-stage channels represent the initial situations before the hydrological model transforms them into the same trapezoidal drainage ditch configuration of the reference site. The magnitude of change applied to both channel depth and associated velocity are an average of those inferred by the model for the specified days. As both cross-sections and velocities are to scale, the effect of the difference in hydraulic roughness between Site 1 and Site 3 at low flow is quite apparent since the effect of local slope is applied to the respective trapezoidal channel flows; hence the lower velocity observed in the trapezoidal channel of the Site 1 scenario. **The combined effect of the overall lower hydraulic roughness and two-floodplain design of the Site 3 scenario is most representative of the potential hydraulic performance of two-stage channel restoration at high flow condition.**

Although the combined influence of higher hydraulic roughness and downstream hydraulic control at high flows partially obscure a definitive assessment of a one vs. two-floodplain design, the simulation still provide insight in potential differences in performance.

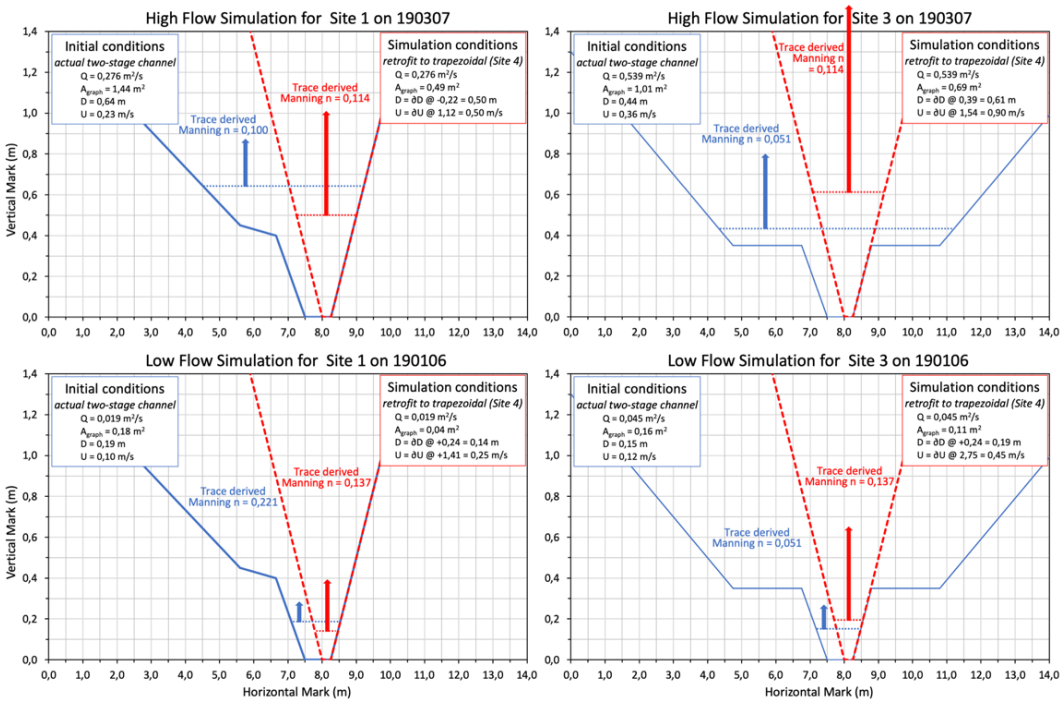

Figure 33 Relative differences in water depths and velocities inferred from the simulation of a low and high flow events that respectively occurred on 30th September and 7th March 2019 in the 3 study-sites. The channel cross-sections are to scale and the length of all arrows is scaled to represent relative velocities.

7 Conclusions and recommendations

7.1.1 Hydraulic performance of two-stage channels

The simulations clearly indicate that, whilst it does not significantly attenuate peak-flow, restoring Site 4 trapezoidal drainage ditch to the Site 3 two-stage two-floodplain channel characteristics significantly decreases both water depth (*ca.* -35% on average) and velocity (*ca.* -160% on average; -1 to -2 folds range) during overbank flow. Although obscured by the joint influence of high hydraulic roughness and downstream hydraulic control of Site 1, the simulation also indicates that performance is less with only one floodplain.

Since simulations also infer that a minimum of 50% reduction (*i.e.*, -1,0 fold) in water velocity at high flows by either a two- or one-floodplain configuration, a two-stage channel restoration approach potentially decreases risks of bank erosion and sediment transport. Substantial increase in hydraulic retention time associated with this velocity reduction also potentially promotes nutrient retention by further trapping particles and providing time for biogeochemical processes.

The simulation also highlights that, if restoration is conducted on reaches with shallow bed-slope, special attention must be provided to pro-actively control in-channel vegetation (*i.e.*, hydraulic roughness) to sustain water depth reduction performance. Furthermore, it highlights that such performance would be even lower if a downstream pond is present (*i.e.*, downstream hydraulic control).

Field observations show that high levels of in-channel "*plant-stabilized sediment*" provokes early overbank flow conditions by reducing the main channel cross-section area. Although localized early overbank spills could be seen as positive (*e.g.*, sediment and nutrient trapping), a generalised over-growth state significantly reduces hydraulic performance at high flows by reducing storage potential. This highlights the importance of creating conditions, either by pre-emptive design and/or planned maintenance, that **maintain low flow velocities high enough to prevent sediment accumulation and impede in-channel vegetation establishment**. As seen in Site 3, extended shading significantly impedes emergent in-channel vegetation. Early tree planting and species selection is therefore part of ensuring the safeguard of the two-stage channel hydraulic performance.

Additionally, field observations during overbank flow also revealed that the great majority of the water rapidly flows downstream in the main-channel portion of the flooded cross-section of the two-stage channel, bypassing the full hydraulic influence of floodplains. As water flows over the floodplains, the effect of hydraulic resistance (*i.e.*, Manning roughness) is applied to the entire surface where water is in contact with the bottom of the cross-section (*i.e.*, the wetted perimeter). The larger the floodplain width, the longer the wetted perimeter. For example, whilst they follow a similar relationship between wetted-perimeter and cross-section area for their main-channel, the two-floodplain Site 3 has a wetted-perimeter *ca.* 1,5 folds longer than that of the one-floodplain Site 1 for an identical cross-section area of 1m^2 (Figure 34). Similarly, Site 3 has a wetted-perimeter almost twice of that of the trapezoidal control channel (Site 4), whilst that of Site 1 is only *ca.* 1,3 folds longer. The lower values in channel wetted-perimeter at Site 4 is due to the initial narrower width of its composite profile (Figure 25).

A key assumption in using a 1-D model to simulate the effect of water flow over floodplains is that the velocity field is uniformly distributed over those floodplains. A similar assumption is made when discussing the potential effect of overbank velocity reduction on erosion and sediment transport, as well as nutrient retention. Field assessment of floodplain phosphorous deposition and reach nutrient retention potential of the Lussebäcken two-stage channel sites has confirmed that the flow-bypass phenomena brought to light by the conservative tracing study (Figure 27) is a significant hindrance to

their performance[‡]. Complementary traces conducted at Site 1 in collaboration with Prof. Ian Guymer (University of Sheffield, UK) suggest that less than 30% of the injected dye actually travels over the floodplain by the time it reaches the 200m mark[§].

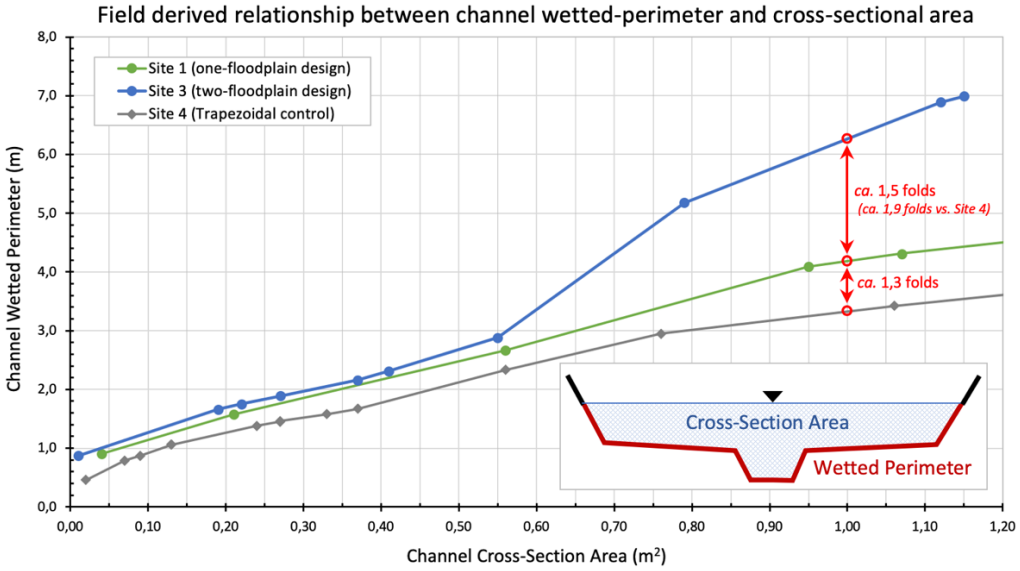

Figure 34 Field derived relationship between wetted-perimeter and cross-section area for the one-floodplain (Site 1), two-floodplain (Site 3) and trapezoidal (Site 4) channels sites.

These findings suggest that, although the hydrological model is a fair representation of the overall hydraulic behaviour of the studied sites, the fact that the velocity field is in reality not uniformly distributed over the floodplains suggest that the actual "field-performance" may be to some extent lower. Similarly, it also indicates that measures recommended to improve particulate and nutrient retention should be tested (*i.e.*, included as "low-head hydraulic control" nodes) in the existing scenarios as to assess to what extent they also secure the two-stage channel designs hydraulic performance.

In accordance to the separately provided report, these are:

- ***supress in-channel plant-sediment feedback process*** *by ensuring early shading of the main-channel and major parts of the floodplains; hence minimising emergent plants growth in the main-channel and promoting grass growth on the floodplains.*

- ***promote early overbank flow*** *by selecting shallower floodplain heights (i.e., slightly reduced main-channel cross-section in relation to the $Q_{1.5}$ dimension). Although caused by partial sediment accumulation, the influence of reduced main channel cross-section is seen at Site 2; whilst the effect of "over-dimension" is apparent in Site 3.*

- ***promote overbank flow frequency and duration*** *by placing/keeping low-head structures (such as riffle-pools or small woody debris-dams) along the entire two-stage channel reach. To optimise their influence, the number and spacing of these structures must be adapted to the reach gradient. The consequence of not retaining such structure is seen in Site 3 low flooding frequency.*

- ***promote transversal mixing between the main-channel and the floodplains*** *by securing deflectors on the bank (e.g., small and short tree logs) at an angle that will spread the flow-field over the entire floodplain. To optimise their influence, these*

[‡] EA International, 2020, *Field evaluation of two-stage channels impact on nutrient retention potential and local biodiversity*, Rapport to The County Board of Skåne (Länsstyrelsen Skåne Län) no 2020:06 (ISBN: 978-91-7675-185-5).

[§] Assessment based on comparing the longitudinal dye flux over the floodplain to that of the main channel.

should be place in tandem with the in-channel low-head structures.

Consequently, in small streams such as Lussebäcken, hydraulic roughness is known to be derived from three possible forms of resistance to water flow. While the first one, *boundary roughness* (channel and floodplain material and vegetation), is present in all types of channels, the second one, *form resistance* (turbulence and circulation generated by channel sinuosity and irregularities) develops through inescapable hydrogeomorphic processes. Finally, naturally present in mature systems, *spill resistance* is induced by rapidly decelerating flows associated with hydraulic jumps induced by elements near or protruding from the water surface such as riffles. The later consequently highlight the actual lack of in-channel structure such as riffles-pools sequences that would, not only contribute to the overall hydraulic resistance of the present two-stage channel designs, but also promote lateral circulation and flow-field distribution over the floodplain at high flows. This also illustrates that, unless low-head structures (such as riffle-pools or small woody debris-dams) are in place to also promote some type of impounding across the entire floodplain and along the entire reach, no significant flow attenuation can be achieved on relatively short restoration reaches.

Finally, the simulations have also indicated that *outlet control* (*i.e.*, friction along the length of a culvert pipe and size of the downstream tailwater depth) can exert significant control over upstream impoundment. Consequently, if flood-peak attenuation is the overriding objective in establishing a two-stage channel, maximizing the volumetric storage over the floodplains can be obtained by reconfiguration of the culvert opening geometry. Optimisation of the outlet would ensure that extreme flows are not impeded, but that a set proportion of the flows is securely detained and slowly released to maximise peak attenuation in the same manner as in an extended detention pond/wetland. As the effect of restoration length has not been estimated at this time and since *outlet control* is the only way to guarantee significant flow attenuation in short restoration reach, future updates of the Lussebäcken hydraulic model should include this option.

7.1.2 Use of conservative-trace data in model calibration/validation process

Overall, the calibrated model of the Lussebäcken study-sites captures quite well the trends and feedbacks over the whole range of conditions observed during the studied time period. Following the adjustment in the profiles of both two-stage channel cross-sections to match the higher resolution survey, a good fit was obtained for Site 1 and an incredibly good fit achieved at Site 3 for low flows and water depths to about 0,3 m. It should be stressed that the required outcome of the model is at a relatively fine resolution (*i.e.*, cm) although the model descriptive resolution is rather coarse; inputs being based on channel longitudinal profiles and cross-sections measured every 30-50 m, with a linear interpolation between these points to depict the channel bottom level. This indicates that a more accurate longitudinal profile of each site would improve model description and reliability.

The validation process, where the outcome of simulated conservative traces (*i.e.*, inferred flow velocities based on the factual distances between injection and recording points) are compared to those obtained from the field traces, confirmed **that trace-derived velocities are good surrogates for automatically-recorded water depth in the calibration of hydraulic resistance in the model**. Improved resolution and reliability at high flows would have gained from a larger number of traces in the upper part of the possible discharge range. This also applies to the trace-derived discharge-stage rating curves.

Finally, in order to more accurately describe the effect from the differences in main-channel and floodplain roughness, further updates of the Lussebäcken hydraulic model should consider using a 2D model instead of the current 1D model. It should also consider seasonal changes in hydraulic roughness; as demonstrated by the outcome of traces performed at the start and height of the autumn in-channel vegetation die-out where, in a 4 weeks span, the trace-derived Manning n doubled in Site 1 (almost tripled in the reference site) while nothing changed in Site 3 as there is no significant in-channel vegetation present.

Annex 1 Summary of trace derived parameters

Lussebäcken Study Sites - Summary of trace derived parameters; where “h” is the stream-stage as recorded by Naturcentrum AB and “Q”, “U” and “D” are respectively Stream Discharge, Average Cross-Sectional Velocity and Dispersion Coefficient. Green shading indicates “vegetated season”. Grey shading indicates extrapolated values of stream stage (h) where recording was not available.

Location Names	Time Stamp	h (m)	Q (l/s)	$\bar{\tau}$ (min)	U (m/s)	D (m^2/s)
Station 1 / BWN 3 / NaturCentrum 1	2018-11-28 03:20:16	0,067	0,11	960,25	0,004	0,018
Station 1 / BWN 3 / NaturCentrum 1	2019-09-30 16:30:58	0,207	22,40	90,03	0,038	0,156
Station 1 / BWN 3 / NaturCentrum 1	2019-10-28 14:20:23	0,391	52,42	131,22	0,026	0,025
Station 1 / BWN 3 / NaturCentrum 1	2019-02-10 10:27:42	0,510	136,33	32,87	0,103	0,357
Station 1 / BWN 3 / NaturCentrum 1	2019-02-09 16:12:51	0,542	131,39	34,35	0,099	0,760
Station 1 / BWN 3 / NaturCentrum 1	2019-03-08 10:48:09	0,586	196,28	26,30	0,139	0,714
Station 1 / BWN 3 / NaturCentrum 1	2019-03-07 16:40:47	0,691	314,94	21,87	0,155	0,672
Station 1 / BWN 3 / NaturCentrum 1	2019-03-17 10:20:07	0,791	412,63	19,87	0,171	0,796
Station 2 / BWN 2 / NaturCentrum 3	2019-09-30 17:30:00	0,109	40,00	191,42	0,020	0,115
Station 2 / BWN 2 / NaturCentrum 3	2019-10-28 15:03:44	0,139	112,57	199,98	0,019	0,004
Station 2 / BWN 2 / NaturCentrum 3	2019-02-09 16:01:44	0,224	105,15	62,23	0,062	0,788
Station 2 / BWN 2 / NaturCentrum 3	2019-02-10 10:48:20	0,243	187,17	71,33	0,054	0,395
Station 2 / BWN 2 / NaturCentrum 3	2019-03-08 11:30:36	0,312	289,09	53,25	0,072	0,882
Station 2 / BWN 2 / NaturCentrum 3	2019-03-07 14:36:28	0,361	349,26	44,47	0,086	1,421
Station 2 / BWN 2 / NaturCentrum 3	2019-03-07 17:38:08	0,361	375,73	46,80	0,082	1,204
Station 2 / BWN 2 / NaturCentrum 3	2019-03-17 11:49:19	0,439	820,73	33,65	0,114	1,501
Station 3 / BWN 1 / NaturCentrum 2	2018-11-27 13:19:12	0,033	0,33	197,20	0,012	0,205
Station 3 / BWN 1 / NaturCentrum 2	2019-09-30 14:02:11	0,165	35,35	22,25	0,106	0,506
Station 3 / BWN 1 / NaturCentrum 2	2019-09-28 12:11:07	0,182	60,86	76,12	0,031	0,006
Station 3 / BWN 1 / NaturCentrum 2	2019-02-08 12:22:50	0,214	81,08	13,33	0,177	2,662
Station 3 / BWN 1 / NaturCentrum 2	2019-02-09 14:01:54	0,263	157,46	9,40	0,250	1,123
Station 3 / BWN 1 / NaturCentrum 2	2019-02-10 09:19:12	0,282	209,56	9,20	0,256	1,762
Station 3 / BWN 1 / NaturCentrum 2	2019-03-08 11:01:55	0,339	403,10	6,75	0,349	0,930
Station 3 / BWN 1 / NaturCentrum 2	2019-03-07 13:22:28	0,403	725,17	6,22	0,378	1,193
Station 3 / BWN 1 / NaturCentrum 2	2019-03-17 12:30:48	0,459	1 165,84	5,30	0,445	1,044
Station 3 / BWN 1 / NaturCentrum 2	2019-03-17 10:46:32	0,463	1 204,16	5,28	0,446	1,187
Station 4 / BWN 4 / NaturCentrum 7	2018-11-27 20:15:09	n/a	0,05	664,13	0,005	0,087
Station 4 / BWN 4 / NaturCentrum 7	2019-09-30 14:23:39	0,069	7,01	66,90	0,053	0,239
Station 4 / BWN 4 / NaturCentrum 7	2019-10-28 12:17:07	0,158	19,60	104,62	0,034	0,006
Station 4 / BWN 4 / NaturCentrum 7	2019-02-08 11:28:51	0,184	23,43	34,35	0,103	0,168
Station 4 / BWN 4 / NaturCentrum 7	2019-02-09 13:19:57	0,238	43,89	27,43	0,129	0,229
Station 4 / BWN 4 / NaturCentrum 7	2019-02-10 09:32:26	0,238	44,09	33,43	0,106	0,151
Station 4 / BWN 4 / NaturCentrum 7	2019-03-08 11:35:50	0,335	81,62	23,17	0,153	0,747
Station 4 / BWN 4 / NaturCentrum 7	2019-03-07 17:26:32	0,362	123,10	19,70	0,180	0,363
Station 4 / BWN 4 / NaturCentrum 7	2019-03-07 12:17:33	0,358	131,13	19,72	0,180	0,474
Station 4 / BWN 4 / NaturCentrum 7	2019-03-17 12:48:27	0,435	189,09	17,03	0,208	0,668
Station 4 / BWN 4 / NaturCentrum 7	2019-03-17 11:15:21	0,405	201,96	17,02	0,209	0,570

Annex 2 Summary of discharge-stage rating curves data

Lussebäcken Study Sites - Summary of the data used in developing the study sites discharge-stage rating curves; where the method indicate how it was derived: Field = Velocity-Area Method, Trace = Conservative Trace with a Time Stamp equal to the Average Travel Time ($\bar{t}$), EA = EA International and NC = Naturcentrum AB. At the exception of values highlighted by a grey cell (see section 4.5), all stage data is provided by NC telemetry. Highlighted green cells = high vegetation condition.

Station 1 / BWN 3 / NaturCentrum 1			
Time Stamp	**Method**	**Q (L/s)**	**h (m)**
2019-08-30 16:00	Field NC	1,0	0,033
2018-11-28 03:20	Trace EA	1,10	0,067
2018-11-28 14:00	Field EA	1,4	0,067
2019-05-08 11:00	Field EA	7,5	0,071
2019-09-19 00:00	Field NC	6,3	0,086
2019-09-27 14:00	Field EA	8,6	0,101
2019-01-07 12:05	Field EA	12,8	0,161
2019-10-01 14:30	Field EA	17,7	0,161
2019-09-30 16:30	Trace EA	22,4	0,207
2019-10-29 09:30	Field EA	35,1	0,361
2019-10-28 14:20	Trace EA	52,4	0,391
2019-02-08 12:00	Field EA	106,1	0,399
2019-02-11 10:00	Field EA	117,3	0,482
2019-02-10 10:27	Trace EA	136,33	0,510
2019-02-09 15:15	Field EA	203,1	0,542
2019-02-09 16:12	Trace EA	131,39	0,542
2019-03-08 12:00	Field EA	160,7	0,580
2019-03-08 10:48	Trace EA	196,28	0,586
2019-03-08 10:00	Field NC	276,9	0,588
2019-03-07 16:40	Trace EA	314,94	0,691
2019-03-17 10:20	Trace EA	412,63	0,791

Station 2 / BWN 2 / NaturCentrum 3			
Time Stamp	**Method**	**Q (L/s)**	**h (m)**
2019-05-08 12:30	Field EA	14,41	0,086
2019-01-07 11:40	Field EA	*12,8*	0,096
2019-09-30 17:30	Trace EA	40,0	0,109
2019-09-27 13:25	Field EA	42,3	0,124
2019-10-28 15:03	Trace EA	112,7	0,139
2019-10-29 10:00	Field EA	38,1	0,141
2019-02-08 12:00	Field EA	*131,20*	0,195
2019-02-09 14:30	Field EA	*209,4*	0,207
2019-02-11 10:00	Field EA	158,0	0,222
2019-02-09 16:01	Trace EA	105,15	0,224
2019-02-10 10:48	Trace EA	187,17	0,243
2019-03-08 12:45	Field EA	243,4	0,297
2019-03-08 11:30	Trace EA	289,09	0,312
2019-03-07 13:30	Field EA	363,5	0,361
2019-03-07 14:36	Trace EA	349,3	0,361
2019-03-07 17:38	Trace EA	375,7	0,361
2019-03-17 11:49	Trace EA	820,73	0,439

Station 3 / BWN 1 / NaturCentrum 2			
Time Stamp	**Method**	**Q (L/s)**	**h (m)**
2018-11-27 13:19	Trace EA	*0,33*	*0,033*
2018-11-28 12:00	Field EA	4,2	0,041
2019-05-08 13:30	Field EA	12,60	0,071
2019-08-30 16:00	Field NC	1,5	0,078
2019-01-07 10:40	Field EA	20,1	0,090
2019-09-19 12:00	Field NC	15,0	0,127
2019-09-30 14:02	Trace EA	35,4	0,165
2019-10-29 10:45	Field EA	58,1	0,173
2019-09-27 14:30	Field EA	63,3	0,180
2019-10-28 12:11	Trace EA	60,9	0,182
2019-02-08 12:00	Field EA	81,90	0,214
2019-02-08 12:22	Trace EA	81,08	0,214
2019-02-11 11:00	Field EA	189,8	0,252
2019-02-09 14:01	Tace EA	157,5	0,263
2019-02-09 13:30	Field EA	183,1	0,271
2019-02-10 09:19	Trace EA	209,6	0,282
2019-03-08 13:30	Field EA	309,4	0,335
2019-03-08 10:00	Field NC	350,0	0,339
2019-03-08 11:01	Trace EA	403,10	0,339
2019-03-07 13:00	Field EA	484,0	0,403
2019-03-07 13:22	Trace EA	725,17	0,403
2019-03-17 12:30	Trace EA	1 165,84	0,459
2019-03-17 10:46	Trace EA	1 204,16	0,463

Station 4 / BWN 4 / NaturCentrum 7			
Time Stamp	**Method**	**Q (L/s)**	**h (m)**
2018-11-27 20:15	Trace EA	0,1	n/a
2018-11-28 14:30	Field EA	0,9	n/a
2019-01-07 11:00	Field EA	3,8	n/a
2019-08-30 16:00	Field NC	0,5	0,010
2019-09-19 12:00	Field NC	0,2	0,010
2019-05-08 12:00	Field EA	3,1	0,022
2019-09-27 15:00	Field EA	12,0	0,060
2019-09-30 14:23	Trace EA	7,1	0,069
2019-10-29 11:20	Field EA	18,6	0,154
2019-10-28 12:17	Trace EA	19,6	0,158
2019-02-08 11:00	Field EA	25,7	0,184
2019-02-08 11:28	Trace EA	23,43	0,184
2019-02-11 11:00	Field EA	44,8	0,224
2019-02-09 13:10	Field EA	49,5	0,238
2019-02-09 13:19	Trace EA	43,89	0,238
2019-02-10 09:32	Trace EA	44,1	0,238
2019-03-08 10:00	Field NC	75,8	0,324
2019-03-08 11:35	Trace EA	81,62	0,335
2019-03-08 11:20	Field EA	90,5	*0,338*
2019-03-07 17:26	Trace EA	123,10	*0,362*
2019-03-07 12:17	Trace EA	131,13	*0,365*
2019-03-17 11:15	Trace EA	202,0	0,405
2019-03-17 12:48	Trace EA	189,1	0,435

Annex 3 Summary of the detailed field survey data

Lussebäcken Study Sites - Summary of the detailed field survey data.

Study Site 1 (top) [BwN lokal 3]

Transect 1

Lat 56.049735° Lon 12.780411°

Start Left Bank Date 191126

X (m)	Z (m)	Comment
0,0	0,970	
0,5	0,874	
1,0	0,805	
1,5	0,723	
2,0	0,676	
2,5	0,637	
3,0	0,527	
3,5	0,500	
4,0	0,480	
4,5	0,399	water edge
4,7	0,391	bank edge
5,0	0,161	
5,5	0,042	
6,0	0,000	
6,2	0,128	
6,7	0,416	water edge
7,0	0,722	
7,5	1,091	
8,0	1,193	

Transect 2

Lat 56.049585° Lon 12.781091°

Start Left Bank Date 191126

X (m)	Z (m)	Comment
0,0	0,985	
0,5	0,886	
1,0	0,845	
1,5	0,772	
2,0	0,700	
2,5	0,647	
3,0	0,635	
3,5	0,606	
3,8	0,592	water surface
4,2	0,507	bank edge
4,3	0,454	
4,5	0,359	
4,7	0,266	
4,9	0,095	
5,0	0,148	top sediment
5,0	0,066	hard bottom
5,3	0,165	top sediment
5,3	0,037	hard bottom
5,5	0,232	top sediment
5,5	0,000	hard bottom
5,8	0,374	
6,1	0,630	water surface
6,3	0,955	
6,5	1,180	
7,0	1,520	

Transect 3

Lat 56.049288° Lon 12.782868°

Start Left Bank Date 191126

X (m)	Z (m)	Comment
0,0	1,081	
0,5	0,979	
1,0	0,871	
1,5	0,766	
2,0	0,617	floodplain edge?
2,5	0,553	
3,3	0,534	water surface
3,6	0,446	bank edge
4,0	0,334	*top sediment*
4,3	0,149	top sediment
4,3	0,064	hard bottom
4,5	0,023	*top sediment*
4,8	0,000	*top sediment*
5,1	0,035	bank edge
5,4	0,193	*top sediment*
5,7	0,504	water surface
6,0	0,916	
6,5	1,343	

Transect 4 (at injection site)

Lat 56.049228° Lon 12.783644°

Start Left Bank Date 191126

X (m)	Z (m)	Comment
0,0	1,097	
0,5	0,945	
1,0	0,804	
1,5	0,601	
2,1	0,481	water surface
2,5	0,389	*top sediment*
3,0	0,353	*top sediment*
3,5	0,321	*top sediment*
3,8	0,313	Full-bank edge
4,0	0,266	*top sediment*
4,3	0,012	*top sediment*
4,5	0,000	*top sediment*
5,0	0,016	*top sediment*
5,3	0,007	*top sediment*
5,7	0,157	*top sediment*
6,0	0,189	*top sediment*
6,5	0,250	*top sediment*
6,7	0,357	*top sediment*
7,3	0,434	water surface
7,6	0,650	Flodplain edge
8,0	0,783	
8,5	0,946	
9,0	1,032	

Transect 5 (NaturCentrum recorder)

Lat 56.049430° Lon 12.781836°

Start Left Bank Date 191107*

X (m)	Z (m)	Comment
0,0	1,710	Vänster sida
1,7	1,380	
3,7	0,995	
5,1	0,665	
5,9	0,465	
6,9	0,320	Vatten nivån
7,8	0,175	Fullbank
8,1	0,060	Kanalens kant
9,0	0,000	Thalweg/sediment
9,9	0,080	sediment
10,1	0,330	
10,4	0,900	
11,2	1,370	
12,9	1,805	Höger sida

* Done by Naturcentrum

Coordinates from Google Earth 2017-06-07 map

STATION 2 (mid) [BwN lokal 2]

OBS: Transect 1, 2 & 3 done with same laser-leveller position

Transect 1

Lat 56.047320° Lon 12.774179°

Start from Left Bar Date 191126

X (m)	Z (m)	Comment
0,0	1,728	
0,5	1,658	
1,0	1,491	
1,5	1,313	
1,8	1,171	
2,2	0,853	Full-bank edge
2,3	0,697	
2,5	0,603	Water surface
3,0	0,417	
3,3	0,323	
3,5	0,262	
3,8	0,232	Bank edge
4,0	0,117	top sediment
4,1	0,063	hard bottom
4,3	0,237	top sediment
4,3	0,093	hard bottom
4,8	0,203	top sediment
4,8	0,121	hard bottom
5,0	0,153	
5,3	0,222	top sediment
5,3	0,042	hard bottom
5,5	0,133	top sediment
5,5	0,000	hard bottom
5,8	0,103	
6,0	0,243	
6,3	0,295	
6,5	0,401	
7,0	0,476	
7,5	0,536	
7,9	0,617	Water surface
8,5	0,855	
9,0	1,023	
9,5	1,185	
10,0	1,390	

Transect 2

Lat 56.047473° Lon 12.774431°

Start from Right Bi Date 191126

X (m)	Z (m)	Comment
0,0	1,606	
0,5	1,418	
1,0	1,227	
1,5	0,967	
2,0	0,806	
2,3	0,636	
2,4	0,538	water surface
3,0	0,389	
3,5	0,323	
3,8	0,262	
4,0	0,233	
4,3	0,178	
4,5	0,196	top sediment
4,5	0,025	hard bottom
5,0	0,138	top sediment
5,0	0,042	hard bottom
5,5	0,000	top=hard
5,8	0,106	channel edge
6,0	0,134	
6,3	0,183	
6,5	0,230	
6,8	0,315	
7,0	0,338	
7,4	0,492	water surface
7,7	0,670	
8,0	0,825	
8,3	1,072	
8,5	1,218	
8,8	1,348	
9,0	1,452	
9,5	1,646	
10,0	1,725	

Transect 3

Lat 56.047184° Lon 12.773950°

Start from Right Bi Date 191126

X (m)	Z (m)	Comment
0,0	1,508	
0,5	1,327	
1,0	1,173	
1,5	0,990	
2,0	0,810	
2,3	0,721	
2,5	0,657	
2,7	0,598	Water surface
3,0	0,552	
3,3	0,524	
3,5	0,478	
4,0	0,359	top sediment
4,0	0,282	hard bottom
4,4	0,411	top sediment
4,4	0,318	hard bottom
5,0	0,342	top sediment
5,0	0,000	hard bottom
5,5	0,223	top sediment
5,5	0,076	hard bottom
6,1	0,148	
6,5	0,248	
7,0	0,322	
7,3	0,320	
7,5	0,393	
7,8	0,460	
8,2	0,620	Water surface
8,5	0,807	
8,8	0,953	
9,0	1,031	
9,5	1,202	
10,0	1,356	
10,5	1,511	
11,0	1,641	
11,5	1,811	

Transect 4

Lat 56.046928° Lon 12.773475°

Start from Left Bar Date 191126

X (m)	Z (m)	Comment
0,0	1,665	
0,5	1,544	
1,0	1,392	
1,5	1,220	
2,0	1,072	
2,1	1,008	
2,4	0,914	
2,6	0,880	water surface
3,0	0,779	
3,3	0,725	
3,5	0,691	
3,8	0,638	
4,0	0,614	
4,5	0,587	
4,9	0,523	
5,3	0,415	
5,5	0,456	top sediment
5,5	0,263	hard bottom
6,0	0,407	top sediment
6,0	0,128	hard bottom
6,5	0,395	top sediment
6,5	0,000	hard bottom
7,0	0,424	top sediment
7,0	0,343	hard bottom
7,3	0,532	
7,5	0,660	
7,8	0,780	
8,0	0,820	
8,7	0,876	water surface
9,0	0,980	
9,5	1,075	
10,0	1,223	
10,5	1,349	
11,0	1,468	
11,5	1,570	

Transect 5 (NaturCentrum recorder)

Lat 56.046680° Lon 12.773062°

Start from Left Bar Date 191107*

X (cm)	Z (m)	Kommentarer
0,0	2,285	Vänster sida
3,4	1,100	
5,0	0,555	
5,6	0,410	
6,3	0,340	
6,9	0,190	Kanten av svämplan
7,5	0,115	
8,0	0,000	
9,0	0,110	
9,6	0,105	Vattendjup över sensorn = 54,5cm
10,1	0,400	
11,5	0,500	Vatten nivån
12,2	0,750	Fullbank
13,2	1,120	
16,0	1,925	Höger sida

* Done by Naturcentrum

Coordinates from Google Earth 8/24/2019 map

STATION 3 (down) [BwN lokal 1]

Transect 1

Lat 56.041126° Lon 12.772602°

Start from Right Bank

X (m)	Z (m)	Comment
0,0	1,330	
0,9	1,160	
1,6	1,025	
2,1	0,738	
2,6	0,603	
3,1	0,555	
3,6	0,467	
3,9	0,394	water surface
4,6	0,378	
5,1	0,424	
5,6	0,394	
6,1	0,319	
6,6	0,338	
7,1	0,477	
7,6	0,414	
7,7	0,074	
7,9	0,017	
8,4	0,032	
8,8	0,000	
9,2	0,264	
9,6	0,374	
10,0	0,401	water surface
10,6	0,473	
11,1	0,528	
11,6	0,526	
12,1	0,549	
12,6	0,541	
13,1	0,573	
13,6	0,615	
14,1	0,665	
14,6	0,702	
15,1	0,820	
15,6	0,798	
16,1	0,957	
16,6	1,055	
17,1	1,150	
17,6	1,290	
18,1	1,335	

Transect 2

Lat 56.041558° Lon 12.772283°

Start from Right Bi Done on 191130

X (m)	Z (m)	Comment
0,0	1,302	
1,0	1,071	
1,5	1,021	
2,0	0,926	
2,5	0,781	
3,0	0,662	
3,5	0,546	
4,0	0,494	
4,5	0,446	
5,0	0,363	
5,5	0,366	
6,0	0,358	
6,5	0,343	
7,0	0,298	
7,5	0,308	
8,0	0,352	
8,7	0,275	water surface
9,0	0,155	
9,3	0,000	
9,5	0,051	
10,0	0,006	
10,4	0,014	
10,8	0,273	water surface
11,0	0,346	
11,5	0,413	
12,0	0,436	
12,5	0,472	
13,0	0,502	
13,5	0,483	
14,0	0,543	
14,5	0,591	
15,0	0,686	
15,5	0,753	
16,0	0,854	
16,5	0,974	
17,0	1,048	
17,5	1,128	
18,0	1,206	
18,5	1,284	
19,0	1,367	

Transect 3

Lat 56.041822° Lon 12.772108°

Start from Right Bi Done on 191130

X (m)	Z (m)	Comment
0,0	1,407	
1,0	1,186	
2,0	1,030	
3,0	0,858	
4,0	0,656	
4,5	0,544	
5,0	0,442	
5,5	0,384	
6,0	0,346	
6,5	0,332	
7,0	0,329	
7,5	0,362	
8,0	0,349	
8,7	0,266	water surface
9,0	0,043	
9,5	0,017	
10,0	0,000	
10,3	0,105	
10,4	0,275	water surface
10,5	0,332	
11,0	0,396	
11,5	0,425	
12,0	0,434	
12,5	0,462	
13,0	0,514	
13,5	0,589	
14,0	0,689	
14,5	0,766	
15,0	0,879	
16,0	1,040	
17,0	1,229	
18,0	1,434	
19,0	1,579	

Transect 4

Lat 56.042025° Lon 12.771990°

Start from Left Bai Done on 191130

X (m)	Z (m)	Comment
0,0	1,328	
1,0	1,203	
2,0	0,958	
3,0	0,818	
4,0	0,651	
5,0	0,515	
5,5	0,432	
6,0	0,415	
6,7	0,349	water surface
6,8	0,109	
7,0	0,033	
7,5	0,003	
8,0	0,000	
8,5	0,057	
8,8	0,113	
9,0	0,142	
9,3	0,277	
9,6	0,344	water surface
10,0	0,380	
10,5	0,351	
11,0	0,380	
11,5	0,350	
12,0	0,360	
12,5	0,389	
13,0	0,396	
14,0	0,553	
15,0	0,720	
16,0	0,935	
17,0	1,138	
18,0	1,348	

Transect 5 (NaturCentrum recorder)

Lat 56.042077° Lon 12.771913°

Start from Left Bai Done on 191107*

X (cm)	Z (m)	Kommentarer
0,0	1,480	Höger sida
2,0	1,070	
4,0	0,665	
5,0	0,520	Kanten av svämplan
6,0	0,415	
7,0	0,455	
8,0	0,370	
8,8	0,265	Vatten nivån
9,3	0,115	
9,8	0,185	
9,9	0,235	Top sensorn
9,9	1,205	Top Peg
9,9	0,000	Botten @ Peg
10,8	0,100	
11,3	0,290	Vatten nivån
12,2	0,460	
13,0	0,540	
14,0	0,720	
15,0	0,930	
17,0	1,310	
19,1	1,780	Vänster sida

* Done by Naturcentrum

Coordinates from Google Earth 12/31/2008 map

STATION 4 (control) [BwN lokal 4]

OBS: all transect (1 to 4) done with same laser-leveller position

Transect 1

Lat 56.041580° Lon 12.764391°

Start from Right B Done on 191130

X (m)	Z (m)	Comment
0,0	2,294	
0,5	2,199	
1,0	1,936	
1,5	1,580	
2,0	1,096	
2,4	0,631	
2,5	0,369	
2,5	0,281	water surface
2,8	0,121	
2,9	0,024	
3,2	0,000	
3,4	0,116	
3,6	0,271	water surface
3,8	0,521	
4,0	0,793	
4,4	1,041	
4,8	1,263	
5,0	1,586	
5,3	1,986	
5,7	2,356	
6,0	2,453	

Transect 2

Lat 56.041756° Lon 12.764358°

Start from Right B Done on 191130

X (m)	Z (m)	Comment
0,0	2,449	
0,7	2,200	
1,0	1,942	
1,3	1,674	
1,5	1,339	
1,9	0,930	
2,1	0,805	
2,2	0,609	
2,5	0,309	water surface
2,7	0,116	
2,9	0,010	
3,1	0,000	
3,4	0,182	
3,6	0,307	water surface
3,7	0,500	
4,1	0,912	
4,4	1,362	
4,8	1,739	
5,2	2,078	
5,5	2,320	
6,0	2,432	

Transect 3

Lat 56.041976° Lon 12.764326°

Start from Right B Done on 191130

X (m)	Z (m)	Comment
0,0	2,452	
0,5	2,277	
0,8	1,967	
1,1	1,680	
1,3	1,442	
1,5	1,222	
1,8	0,977	
2,0	0,782	
2,4	0,545	
2,5	0,398	
2,6	0,345	water surface
2,9	0,167	
3,0	0,005	
3,4	0,000	
3,9	0,322	water surface
4,0	0,602	
4,4	0,885	
4,8	1,267	
5,2	1,637	
5,5	1,897	
6,0	2,250	
6,5	2,517	

Transect 4

Lat 56.042277° Lon 12.764277°

Start from Right B Done on 191130

X (m)	Z (m)	Comment
0,0	2,480	
0,5	2,335	
1,0	1,955	
1,5	1,636	
1,9	1,325	
2,0	1,135	
2,3	0,870	
2,4	0,640	
2,6	0,360	water surface
2,9	0,210	
3,4	0,000	
3,7	0,164	
3,9	0,367	water surface
4,2	0,646	
4,5	1,158	
4,8	1,420	
5,0	1,705	
5,5	2,180	
6,0	2,290	

Transect 5 (NaturCentrum recorder)

Lat xx Lon xx Done on 191107*

X (cm)	Z (m)	Kommentarer
0,0	2,290	Höger sida
0,8	2,250	
1,5	1,800	
2,3	1,150	
2,8	0,845	Kanten av svämplan
3,1	0,380	
3,6	0,215	Vatten nivån
3,9	0,000	
3,9	0,215	Top sensorn
3,9	0,000	
4,6	0,235	Vatten nivån
5,1	0,660	
5,9	1,460	
6,8	2,165	Botten @ Peg
7,7	2,660	Vänster sida

* Done by Naturcentrum

Coordinates from Google Earth 12/31/2008 map

Annex 4 Summary of composite cross-sections data

Data used in the computation of composite cross-sections (see section 4.6.2), which form the basis for Manning n roughness (Equation 2).

Study Site 1 (top) [BwN lokal 3]

X-std (m)	Z1 (m)	Z2 (m)	Z3 (m)	Z4 (m)	Z5 (m)	Z-avr (m)	Z-avr +std	Z-avr -std
-5,10	0,850	0,960	1,150	1,160	0,940	1,012	1,149	0,875
-4,50	0,755	0,860	1,025	0,975	0,810	0,885	0,998	0,772
-3,90	0,685	0,790	0,905	0,805	0,665	0,770	0,868	0,672
-3,30	0,637	0,700	0,775	0,580	0,515	0,641	0,743	0,540
-3,00	0,570	0,670	0,695	0,515	0,450	0,580	0,683	0,477
-2,70	0,520	0,645	0,610	0,450	0,405	0,526	0,628	0,424
-2,40	0,505	0,640	0,575	0,390	0,365	0,495	0,613	0,377
-2,10	0,490	0,625	0,550	0,370	0,320	0,471	0,597	0,345
-1,80	0,480	0,605	0,540	0,344	0,275	0,449	0,586	0,312
-1,50	0,430	0,585	0,535	0,330	0,225	0,421	0,568	0,274
-1,20	0,395	0,525	0,460	0,315	0,175	0,374	0,510	0,238
-0,90	0,235	0,410	0,360	0,265	0,060	0,266	0,401	0,131
-0,60	0,115	0,265	0,200	0,010	0,040	0,126	0,233	0,019
-0,30	0,040	0,150	0,025	0,000	0,020	0,047	0,106	-0,012
0,00	**0,015**	**0,165**	**0,000**	**0,012**	**0,000**	**0,038**	**0,110**	**-0,033**
0,30	0,065	0,260	0,035	0,010	0,030	0,080	0,183	-0,023
0,60	0,250	0,475	0,195	0,075	0,055	0,210	0,379	0,041
0,90	0,460	0,870	0,470	0,165	0,135	0,420	0,717	0,123
1,20	0,720	1,180	0,855	0,200	0,575	0,706	1,067	0,345
1,50	0,930	1,358	1,105	0,235	0,960	0,918	1,335	0,500
1,80	1,110	1,558	1,357	0,355	1,105	1,097	1,553	0,641
2,10	1,155	1,757	1,605	0,400	1,302	1,244	1,772	0,715

STATION 3 (down) [BwN lokal 1]

X-std (m)	Z1 (m)	Z2 (m)	Z3 (m)	Z4 (m)	Z5 (m)	Z-avr (m)	Z-avr +std	Z-avr -std
-7,10	1,070	0,740	0,945	1,250	0,885	0,978	1,171	0,785
-6,10	0,670	0,525	0,760	1,055	0,685	0,739	0,935	0,543
-5,10	0,515	0,415	0,545	0,870	0,535	0,576	0,748	0,404
-4,50	0,390	0,365	0,430	0,785	0,465	0,487	0,658	0,316
-3,90	0,380	0,360	0,370	0,680	0,420	0,442	0,577	0,307
-3,30	0,417	0,240	0,335	0,600	0,440	0,406	0,540	0,273
-2,70	0,385	0,300	0,330	0,515	0,430	0,392	0,477	0,307
-2,10	0,325	0,325	0,360	0,430	0,380	0,364	0,408	0,320
-1,80	0,335	0,355	0,355	0,415	0,340	0,360	0,392	0,328
-1,50	0,405	0,320	0,335	0,395	0,300	0,351	0,398	0,304
-1,20	0,460	0,290	0,300	0,365	0,245	0,332	0,415	0,249
-0,90	0,435	0,190	0,250	0,170	0,170	0,243	0,355	0,131
-0,60	0,070	0,000	0,040	0,025	0,100	0,047	0,086	0,008
-0,30	0,021	0,050	0,025	0,010	0,040	0,029	0,045	0,013
0,00	**0,030**	**0,025**	**0,015**	**0,000**	**0,000**	**0,014**	**0,028**	**0,000**
0,30	0,015	0,005	0,000	0,000	0,045	0,013	0,032	-0,006
0,60	0,095	0,015	0,065	0,030	0,080	0,057	0,091	0,023
0,90	0,260	0,190	0,330	0,070	0,135	0,197	0,299	0,095
1,20	0,360	0,345	0,370	0,130	0,255	0,292	0,393	0,191
1,50	0,385	0,385	0,405	0,260	0,330	0,353	0,412	0,294
1,80	0,415	0,420	0,420	0,330	0,380	0,393	0,432	0,354
2,10	0,450	0,430	0,430	0,365	0,440	0,423	0,456	0,390
2,70	0,520	0,475	0,450	0,355	0,510	0,462	0,528	0,396
3,30	0,525	0,500	0,500	0,380	0,590	0,499	0,575	0,423
3,90	0,545	0,505	0,585	0,350	0,700	0,537	0,664	0,410
4,50	0,557	0,570	0,700	0,370	0,825	0,604	0,775	0,434
5,10	0,600	0,670	0,815	0,395	0,950	0,686	0,897	0,475
6,10	0,690	0,920	0,995	0,520	1,140	0,853	1,100	0,606
7,10	0,840	1,125	1,175	0,690	1,340	1,034	1,298	0,770

Annex 4 *cont.*

STATION 4 (control) [BwN lokal 4]

X-std (m)	Z1 (m)	Z2 (m)	Z3 (m)	Z4 (m)	Z5 (m)	Z-avr (m)	Z-avr +std	Z-avr -std
-1,30	1,39	1,09	0,86	1,10	0,97	1,08	1,28	0,88
-1,20	1,29	0,99	0,78	0,99	0,91	0,99	1,18	0,80
-1,10	1,19	0,90	0,71	0,88	0,85	0,91	1,08	0,73
-1,00	1,09	0,84	0,65	0,73	0,69	0,80	0,98	0,62
-0,90	0,96	0,74	0,58	0,59	0,53	0,68	0,85	0,50
-0,80	0,83	0,62	0,49	0,44	0,38	0,55	0,73	0,37
-0,70	0,70	0,52	0,39	0,34	0,35	0,46	0,61	0,30
-0,60	0,50	0,42	0,32	0,29	0,32	0,37	0,46	0,28
-0,50	0,26	0,34	0,26	0,24	0,28	0,27	0,31	0,24
-0,40	0,21	0,23	0,20	0,20	0,25	0,22	0,24	0,19
-0,30	0,15	0,12	0,11	0,15	0,22	0,15	0,19	0,10
-0,24	0,11	0,07	0,05	0,12	0,17	0,10	0,15	0,06
-0,18	0,05	0,03	0,01	0,09	0,13	0,06	0,11	0,01
-0,12	0,02	0,01	0,00	0,06	0,09	0,04	0,07	0,00
-0,06	0,02	0,01	0,00	0,03	0,04	0,02	0,03	0,00
0,00	0,01	0,00	0,00	0,00	0,00	0,00	0,01	0,00
0,06	0,01	0,00	0,00	0,03	0,02	0,01	0,02	0,00
0,12	0,00	0,02	0,00	0,05	0,04	0,02	0,04	0,00
0,18	0,02	0,05	0,00	0,08	0,06	0,04	0,07	0,01
0,24	0,06	0,08	0,04	0,11	0,08	0,07	0,10	0,04
0,30	0,08	0,13	0,07	0,14	0,10	0,10	0,13	0,07
0,40	0,15	0,19	0,14	0,20	0,14	0,16	0,19	0,13
0,50	0,23	0,26	0,22	0,31	0,17	0,24	0,29	0,18
0,60	0,33	0,34	0,29	0,42	0,21	0,32	0,39	0,24
0,70	0,44	0,50	0,41	0,53	0,24	0,42	0,54	0,31
0,80	0,56	0,61	0,59	0,64	0,32	0,54	0,67	0,42
0,90	0,67	0,71	0,68	0,78	0,40	0,65	0,79	0,50
1,00	0,79	0,81	0,76	0,93	0,49	0,76	0,92	0,59
1,10	0,86	0,91	0,85	1,15	0,57	0,87	1,07	0,66
1,20	0,93	1,06	0,93	1,26	0,66	0,97	1,19	0,75
1,30	1,00	1,22	1,00	1,37	0,76	1,07	1,30	0,84

Annex 5 Summary of trace-derived Manning roughness data

Calculated variables used to assess trace-derived Manning roughness n for 2 two-stage channel site (Site 1 and 3) and the trapezoidal reference site (Site 4). The value of Manning roughness M (1/n) is also provided for ease of comparison with the Swedish literature. At the exception of values highlighted by a grey cell (see section 4.5), all stage data is provided by NC telemetry. Highlighted green cells = high vegetation condition.

Time Stamp	Site	Q	h	A	P	R	S	V	n	M
2018-11-28 03:20	1 (top)	1,10	0,067	0,040	0,900	0,04	0,0010	0,004	1,012	0,99
2019-09-30 16:30	1 (top)	22,4	0,207	0,210	1,580	0,13	0,0010	0,038	0,221	4,53
2019-10-28 14:20	1 (top)	52,4	0,391	0,560	2,670	0,21	0,0010	0,026	0,439	2,28
2019-02-10 10:27	1 (top)	136,33	0,510	0,950	4,090	0,23	0,0010	0,103	0,118	8,46
2019-02-09 16:12	1 (top)	131,39	0,542	1,070	4,310	0,25	0,0010	0,099	0,129	7,75
2019-03-08 10:48	1 (top)	196,28	0,586	1,260	4,590	0,27	0,0010	0,139	0,098	10,21
2019-03-07 16:40	1 (top)	314,94	0,691	1,750	5,260	0,33	0,0010	0,155	0,100	10,03
2019-03-17 10:20	1 (top)	412,63	0,791	2,270	5,930	0,38	0,0010	0,171	0,099	10,06
2018-11-27 13:19	3 (dwn)	*0,33*	*0,033*	*0,010*	*0,870*	0,01	0,0045	0,012	0,310	3,23
2019-09-30 14:02	3 (dwn)	35,4	0,165	0,190	1,660	0,11	0,0045	0,106	0,149	6,72
2019-10-28 12:11	3 (dwn)	60,9	0,182	0,220	1,750	0,12	0,0045	0,131	0,128	7,83
2019-02-08 12:22	3 (dwn)	81,08	0,214	0,270	1,890	0,14	0,0045	0,177	0,105	9,57
2019-02-09 14:01	3 (dwn)	157,5	0,263	0,370	2,160	0,17	0,0045	0,25	0,083	12,12
2019-02-10 09:19	3 (dwn)	209,6	0,282	0,410	2,310	0,18	0,0045	0,256	0,082	12,12
2019-03-08 11:01	3 (dwn)	403,10	0,339	0,550	2,880	0,19	0,0045	0,349	0,064	15,71
2019-03-07 13:22	3 (dwn)	725,17	0,403	0,790	5,180	0,15	0,0045	0,378	0,051	19,69
2019-03-17 12:30	3 (dwn)	1 165,84	0,459	1,120	6,890	0,16	0,0045	0,445	0,045	22,16
2019-03-17 10:46	3 (dwn)	1 204,16	0,463	1,150	6,990	0,16	0,0045	0,446	0,045	22,07
2018-11-27 20:15	4 (ref)	0,1	n/a							
2019-09-30 14:23	4 (ref)	7,1	0,069	0,020	0,460	0,04	0,0040	0,053	0,137	7,32
2019-10-28 12:17	4 (ref)	19,6	0,158	0,070	0,790	0,09	0,0040	0,034	0,367	2,73
2019-02-08 11:28	4 (ref)	23,43	0,184	0,090	0,870	0,1	0,0040	0,103	0,133	7,52
2019-02-09 13:19	4 (ref)	43,89	0,238	0,130	1,060	0,13	0,0040	0,129	0,123	8,13
2019-02-10 09:32	4 (ref)	44,1	0,238	0,130	1,060	0,13	0,0040	0,106	0,150	6,68
2019-03-08 11:35	4 (ref)	81,62	0,335	0,240	1,380	0,17	0,0040	0,153	0,128	7,83
2019-03-07 12:17	4 (ref)	131,13	*0,358*	*0,270*	*1,450*	0,18	0,0040	0,18	0,114	8,80
2019-03-07 17:26	4 (ref)	123,10	*0,362*	*0,270*	*1,460*	0,18	0,0040	0,18	0,113	8,81
2019-03-17 11:15	4 (ref)	202,0	0,405	0,330	1,580	0,21	0,0040	0,209	0,105	9,49
2019-03-17 12:48	4 (ref)	189,1	0,435	0,370	1,670	0,22	0,0040	0,208	0,111	9,05